



AFRL-AFOSR-UK-TR-2019-0020

STARBROOK EXPRESS: Dynamic Calibration of Sensor Measurements
for Near Real-time Space Object Tracking and Characterization

John Paffett
APPLIED SPACE SOLUTIONS LIMITED
20-22 Wenlock Road
LONDON, N1 7GU
GB

04/16/2019
Final Report

DISTRIBUTION A: Distribution approved for public release.

Air Force Research Laboratory
Air Force Office of Scientific Research
European Office of Aerospace Research and Development
Unit 4515 Box 14, APO AE 09421

DISTRIBUTION A: Distribution approved for public release distribution unlimited

REPORT DOCUMENTATION PAGE			<i>Form Approved</i> <i>OMB No. 0704-0188</i>		
<p>The public reporting burden for this collection of information is estimated to average 1 hour per response, including the time for reviewing instructions, searching existing data sources, gathering and maintaining the data needed, and completing and reviewing the collection of information. Send comments regarding this burden estimate or any other aspect of this collection of information, including suggestions for reducing the burden, to Department of Defense, Executive Services, Directorate (0704-0188). Respondents should be aware that notwithstanding any other provision of law, no person shall be subject to any penalty for failing to comply with a collection of information if it does not display a currently valid OMB control number.</p> <p>PLEASE DO NOT RETURN YOUR FORM TO THE ABOVE ORGANIZATION.</p>					
1. REPORT DATE (DD-MM-YYYY) 16-04-2019		2. REPORT TYPE Final		3. DATES COVERED (From - To) 15 Dec 2017 to 14 Dec 2018	
4. TITLE AND SUBTITLE STARBROOK EXPRESS: Dynamic Calibration of Sensor Measurements for Near Real-time Space Object Tracking and Characterization			5a. CONTRACT NUMBER FA9550-18-C-0002		
			5b. GRANT NUMBER		
			5c. PROGRAM ELEMENT NUMBER 61102F		
6. AUTHOR(S) John Paffett			5d. PROJECT NUMBER		
			5e. TASK NUMBER		
			5f. WORK UNIT NUMBER		
7. PERFORMING ORGANIZATION NAME(S) AND ADDRESS(ES) APPLIED SPACE SOLUTIONS LIMITED 20-22 Wenlock Road LONDON, N1 7GU GB			8. PERFORMING ORGANIZATION REPORT NUMBER		
9. SPONSORING/MONITORING AGENCY NAME(S) AND ADDRESS(ES) EOARD Unit 4515 APO AE 09421-4515			10. SPONSOR/MONITOR'S ACRONYM(S) AFRL/AFOSR IOE		
			11. SPONSOR/MONITOR'S REPORT NUMBER(S) AFRL-AFOSR-UK-TR-2019-0020		
12. DISTRIBUTION/AVAILABILITY STATEMENT A DISTRIBUTION UNLIMITED: PB Public Release					
13. SUPPLEMENTARY NOTES					
14. ABSTRACT Results of this research demonstrate an automated near-real-time assessment of measurement biases with an unscented Schmidt Kalman filter. This method has been assessed and quantified by both simulated and measured data. This method will enable the exploitation of so-called 'non-traditional' sensor data to maximize space situational awareness and improve orbital safety.					
15. SUBJECT TERMS Astrodynamics, Space Track					
16. SECURITY CLASSIFICATION OF:			17. LIMITATION OF ABSTRACT SAR	18. NUMBER OF PAGES	19a. NAME OF RESPONSIBLE PERSON MILLER, KENT
a. REPORT Unclassified	b. ABSTRACT Unclassified	c. THIS PAGE Unclassified			19b. TELEPHONE NUMBER (Include area code) 011-44-1895-616022



Optical Express: Dynamic calibration of sensor measurements for near real-time space object tracking and characterisation

Final Report
15th December 2017 – 14th December 2018

Principle Investigator: Dr. John Paffett
Institution: Applied Space Solutions Limited
Address: Building A2, Cody Technology Park,
Old Ively Road, Farnborough,
Hampshire, GU14 0LX, UK.

Contract Number: FA9550-18-C-0002
Program Officer: Dr. Kent Miller AFOSR/IOE



Contents

1	Abstract.....	4
2	Introduction	4
3	Research objectives.....	5
4	Background on metric performance	6
4.1	Metrics for Performance Assessment	6
4.2	Concept of Implementation (CONIMPS)	11
5	Optical data collection and calibration	12
5.1	Errors in RSO Tracking and Processing	12
5.2	The Calibration Process	13
5.3	DEIMOS Data Collection	16
5.4	Non Real-time Calibration Results.....	18
6	Unscented Schmidt Kalman Filter formulation	19
6.1	USKF Background	19
6.2	Consider Parameter Implementation.....	20
6.3	Use of Fisher Information.....	21
6.4	Estimated vs. Consider State Implementation	21
6.5	USKF Time Bias Formulation	22
7	Dynamic calibration results.....	23
7.1	Analysis Background.....	23
7.2	Two-Satellites and Two-Sensors Simulation Results	24
7.3	Real Data Single-Satellite and Single-Sensor	30
8	Dynamic calibration analysis results for multiple satellites and sensors	33
8.1	Analysis Scenario Background	33
8.2	Analysis Results for when Reference Satellite is Included in the Filter	35
8.3	Analysis Results for when No Reference Satellite is Included in the Filter	42
9	Discussion of data management for automated real-time implementation.....	44



10	Dissemination.....	45
11	Transition and exploitation	46
12	Future work.....	46
13	Conclusions	47
14	References.....	48
15	Acronyms and abbreviations.....	50
16	Annex – Conference and journal papers	51

1 Abstract

The management of objects in Earth orbit, regardless of the status or mission, relies on timely and actionable observations to maintain so-called “custody” of all trackable Resident Space Objects (RSOs), including space debris, that might pose a hazard to safe, secure, and sustainable operations. For operations in and around the Geosynchronous Earth Orbit (GEO) regime, electro-optical (EO) observations are the most prevalent observation type available for tracking and determining RSO orbits. The quality (both accuracy and precision) of the data affects the inferable kinematic, physical, and other characteristics of RSOs and, in particular, measurement biases will result in inaccurate orbital trajectories and subsequent predictions. Results presented in this report demonstrate an automated near real-time (NRT) assessment of measurement biases with an appropriately implemented Unscented Schmidt Kalman Filter (USKF). The method that is established and presented herein is assessed and quantified using both simulated and actual measurement data. This method will enable the exploitation and mining of so-called “non-traditional” sensor data to maximize Space Situational Awareness (SSA) in a robust and timely fashion toward improvement of orbital safety. The ultimate goal is to provide decision-making evidence required solve problems preventing the space domain from being safe, secure, and sustainable.

2 Introduction

There is a growing need to supplement the existing space surveillance sensor networks with additional sensors to support tracking and management of the ever-increasing population of both active and inactive Earth orbiting RSOs in and near the geosynchronous Earth orbit (GEO) regime [1, 2, 3]. A globally distributed network ensures timely and actionable monitoring of the space domain to help maximize safe use of space for communications, commerce, defence and scientific Earth resources monitoring. There is a need for rapid validation and near real-time (NRT) data integrity monitoring to facilitate rapid, confident, and appropriately weighted incorporation of new or upgraded sensors into a network. Not all sensors tracking RSOs in the GEO regime have ready access to reference satellites (i.e. fiducials) needed for sensor calibration, hence, this work proposes an approach to enable a robust and dynamic globally accessible means for sensor data validation.

The process for adding external third party electro-optic sensors to the space surveillance architecture is lengthy, often making it difficult for the space surveillance practitioner or operator to utilize observational data from external sensors. One of the issues is the ability to characterize and trust the information from the external sensors. The following research was stimulated to identify techniques for the rapid and dynamic calibration of third-party sensors.

This report presents results of a research initiative, funded by the European Office of Aerospace Research and Development (EOARD). A baseline set of EO sensor data, which included known reference RSOs, was analysed to establish a set of training data for the automated NRT sensor calibration and quality assessment. A dynamic Kalman-like filter implementation was developed which uses the NRT estimation of sensor noise and bias characteristics and includes facilitation of a NRT reference satellite orbit state to facilitate the sensor calibration. Sensitivity to unmodeled error sources via so-called Consider Covariance Analysis is also examined. The performance results are demonstrated with measurement data from a single sensor (DEIMOS), with limitations; improvements to results are anticipated when multiple sensors are generating positive detections. The fusion of multiple data types and sources will also maximize the distinction between filter “artefacts” (e.g. apparent but not actual trajectory structure) due to data quality and anomalies versus un-modelled dynamics of the tracked objects in the estimation filter [4]. The research was conducted by Applied Space, L3-ADS and the University of Texas at Austin, and EO tracking data was provided by DEIMOS Space.

3 Research objectives

The primary goal of this research was to investigate, develop and demonstrate a “unified” implementation of an estimation filter that would support accurate and near real-time (dynamic) calibration of electro-optical sensors. This goal can be subdivided into the following objectives:

1. *Develop and propose a Concept of Implementation (CONIMP) for the NRT dynamic calibration and data integrity assessment. The test data collected to support development is presented in § 3 along with metric calibration results computed using current (non-dynamic non-real-time) post-processing techniques*
2. *Research and develop state-of-the-art algorithms in the filtering and fusion of optical data for establishing a dynamic and automated near real-time process for performing “data integrity”, enabling the quality of sensors to be determined and adjusted dynamically as reference and sensor data become available.*
3. *Determine and attribute errors resulting from dynamic mis-modeling versus the measurement related inconsistencies.*
4. *Accommodate shared data and filter products in an archive available in the US and UK to facilitate current and future research activities.*
5. *Provide unclassified calibration of third party electro-optic sensor filter developed and validated using simulated data and further validated with real data.*

4 Background on metric performance

4.1 Metrics for Performance Assessment

There are a number of specific analytical tools that can be exploited as a part of the measurement data integrity process, most of which implement the same models and algorithms that are used in orbit determination (OD) and prediction processing. These techniques, which can be exercised in conjunction with the OD process, are summarized as follows [5]:

Pre-fit residual check (Figure 1): Estimated states and uncertainties are propagated to a measurement time and residuals with respect to the state are computed. These error residuals (differences between actual and predicted observations) are checked to see whether or not they are contained within the expected measurement uncertainty derived from the propagated state uncertainties mapped to the reference frame of the measurements, augmented by the measurement noise statistics. This is also commonly known as the innovations covariance. Dynamic errors can also cause anomalous pre-fit residuals.

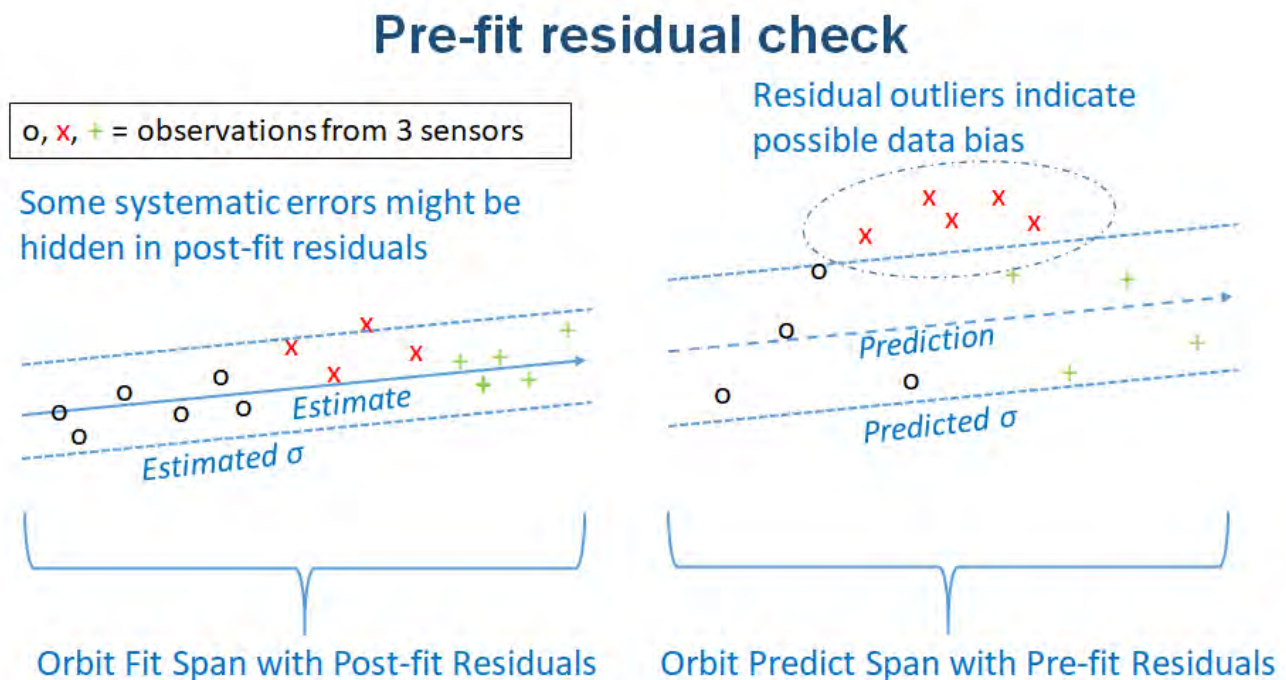


Figure 1. Pre-fit residual check

Post-fit residual check (Figure 2): Ideally, after measurement data are used to infer an orbit, the measurement residuals with respect to the inferred orbital state estimate at the measurement times should be characterized as being purely random (i.e. aleatory uncertainty) if all sources of epistemic uncertainty have been properly accounted for and removed. Any bias or systematic error in the data may otherwise be evident. Unaccounted for dynamic errors can also cause anomalous post-fit residuals. Data anomalies in EO data are typically caused by specific sensor behaviour, in addition to environmental influences and possibly variations due to RSO attitude dynamics.

Post-fit residual check

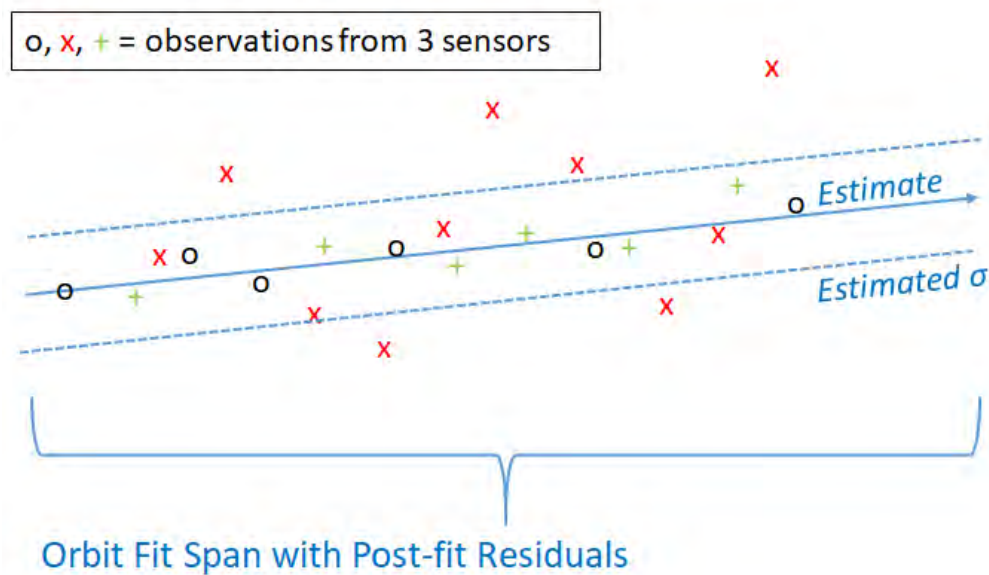


Figure 2. Post-fit residual check

Variable length state estimate comparisons (Figure 3): This metric infers orbits from each independent data set and uses a comparison metric (e.g. Mahalanobis Distance [6]) to assess whether the differences are consistent with the combined uncertainties¹.

¹ We assume Gaussian statistics and therefore implement a Chi-Squared test for this check.

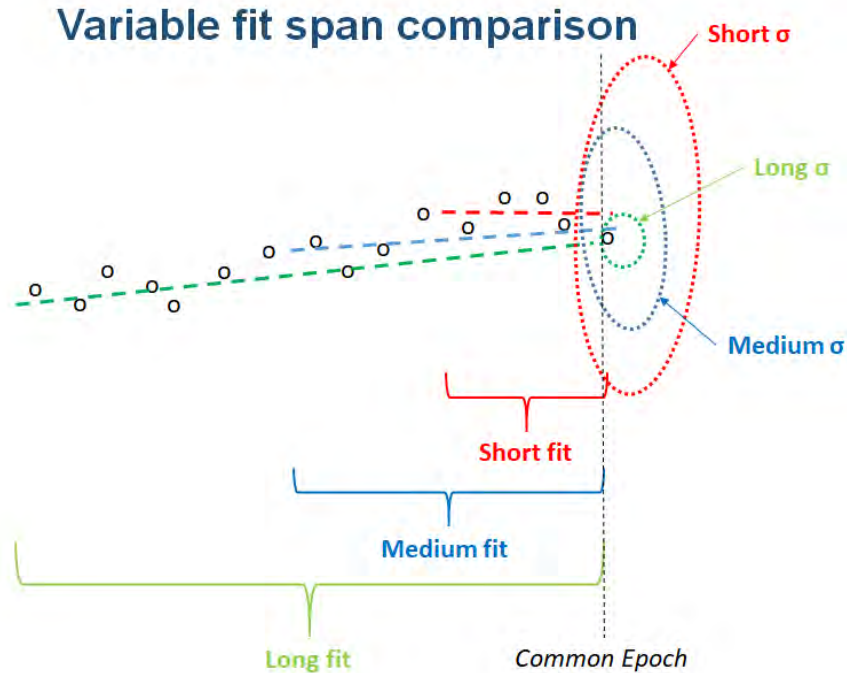


Figure 3. Variable length state estimate comparisons

Independent orbit overlap check (Figure 4): For this quality assessment metric, one or more measurement data sets over distinct and independent spans of measurement data are used to infer independent orbit estimates. These estimates are cross-propagated and their differences are compared with the combined uncertainties. A Mahalanobis Distance (MD) metric can be used as a measure of statistical consistency [6].

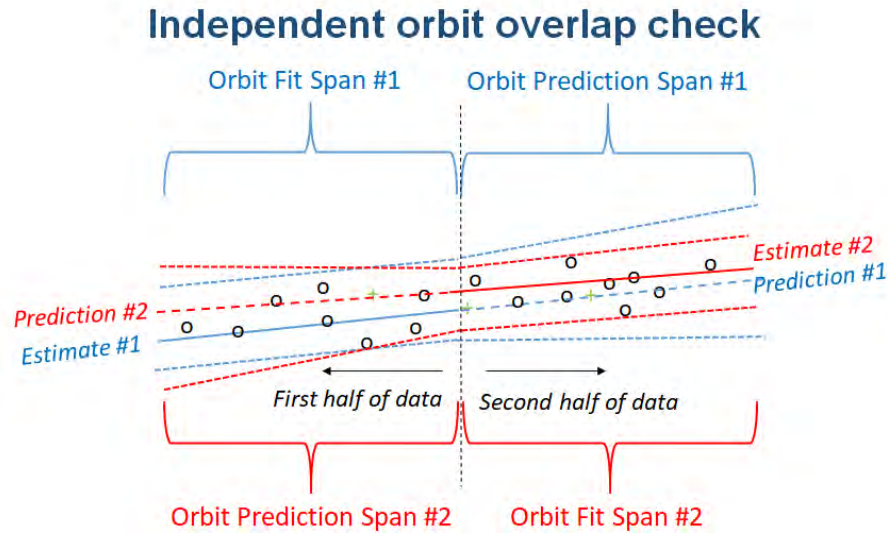


Figure 4. Independent orbit overlap check

Filter-smoother consistency test (Figure 5): When a forward filter backward smoother estimation process is implemented such as the Rauch-Tung-Striebel method [7], the filter-smoother differences in the context of the combined uncertainties can be used as an indication of measurement and/or dynamic inconsistencies present.

Consistency is dependent on measurement data type, quality, and filter modeling assumptions. An example of consistency and lack thereof is shown in Table 1 and can be summarized in the Flock1C 10 satellite example [8]:

- The Flock1C 10 satellite orbit is derived from four independent data sources
- Some estimated parameters are consistent between the sources
 - Semi-major axis (period)
 - Inclination
 - Mean motion
 - Orbital speed
- More variation in derived drag (modeling and observability?)
- Modeling and OD limits the ASTRIA² results

² <http://astria.tacc.utexas.edu/AstriaGraph>

An example of how consistency can be used to assess OD performance is presented in [9].

McReynolds' consistency check

Define the State and Covariance:

$$X_k^f = \text{filtered state estimate at time } t_k$$

$$X_k^s = \text{smoother state estimate at time } t_k$$

$$P_k^f = \text{filtered covariance estimate at time } t_k$$

$$P_k^s = \text{smoother covariance estimate at time } t_k$$

Form the State and Covariance Differences:

$$X_{\Delta k} = X_k^f - X_k^s$$

$$P_{\Delta k} = P_k^f - P_k^s$$

- If $\text{abs}(R_k^i) \leq 3$ for all i and k , then the test is satisfied globally for each estimate
- If $\text{abs}(R_k^i) > 3$ for all i and k , then the filter-smoother test fails globally indicating the possibility of modeling inconsistencies
- Thus, position, velocity and A/m estimation performance can be assessed in terms of the ratio of the estimates to the predicted/assumed modeling uncertainties.

Define the Consistency Ratio:

$$R_k^i = \frac{X_{\Delta k}^i}{\sigma_{\Delta k}^i}$$

Figure 5. Filter-smoother consistency test

Table 1. Example of consistency and inconsistency

FLOCK 1C 10		FLOCK 1C 10	
Data Source	(1) USSTRATCOM	Data Source	(2) Planet
Name	FLOCK 1C 10	Name	FLOCK 1C 10
Country	US	Country	US
Catalog ID	40023	Data epoch	2018-09-02T23:00:01.000Z
Launch date	2014-06-19	Semi-major axis	6984.3 km
Data epoch	2018-09-02T19:46:04.781Z	Eccentricity	0.0010
Semi-major axis	6984.3 km	Inclination	97.9375°
Eccentricity	0.0010	RA of ascending node	163.0866°
Inclination	97.9381°	Argument of perigee	3.1166°
RA of ascending node	162.9516°	Mean motion	0.0620 1/s
Argument of perigee	1.7607°	Orbital speed	7.6 km/s
Mean motion	0.0620 1/s	Orbital period	96.8 min
Orbital speed	7.6 km/s	Ballistic coefficient	5.71 cm ² /kg
Orbital period	96.8 min		
Ballistic coefficient	5.71 cm ² /kg		

FLOCK 1C 10		FLOCK 1C 10	
Data Source	(3) LeoLabs	Data Source	(4) Astria OD/LeoLabs data
Name	FLOCK 1C 10	Name	FLOCK 1C 10
Country	US	Country	US
Data epoch	2018-09-02T23:00:01.000Z	Data epoch	2018-09-02T23:00:01.000Z
Semi-major axis	6984.3 km	Semi-major axis	6764.5 km
Eccentricity	0.0010	Eccentricity	0.0225
Inclination	97.9373°	Inclination	97.5853°
RA of ascending node	163.0874°	RA of ascending node	163.0163°
Argument of perigee	3.2261°	Argument of perigee	245.3607°
Mean motion	0.0620 1/s	Mean motion	0.0850 1/s
Orbital speed	7.6 km/s	Orbital speed	7.9 km/s
Orbital period	96.8 min	Orbital period	92.3 min
Drag coefficient	0.0546	Drag coefficient	1.7152

Other means of assessing data quality involve including parametric combinations of data from a diverse set of sensors. Assuming at least some of the data have been previously calibrated to establish an *a priori* expectation of sensor data performance, the above listed “rules” are used in various combinations of data processing to quantify and assess sensor data performance and consistency. The process is designed to determine the expected NRT performance of the data and orbit products and, where appropriate, detect and identify anomalous data from specific sensors. It is the main goal of this project to work towards this end.

4.2 Concept of Implementation (CONIMPS)

The Defense Advanced Research Projects Agency (DARPA) Orbit Outlook (O2) project [10] was established with the purpose of exploring how to integrate non-traditional sensor data from different sources. We extend O2 capabilities in this work to include additional analytical tools and processes presented herein.

The orbit determination and prediction process is a foundational capability of data integrity processing. It assumes (a) *a priori* knowledge of the data (measurement) noise and their statistics, (b) measurement biases have been accounted for, as well as (c) the appropriate fidelity of the dynamic models being used for the estimation and prediction. In reality, any combination of these assumptions can be invalid; establishing a causal relationship for an unexpected behaviour in the sensor data processing can be challenging due to ambiguities in the possible information and modelling sources and how they manifest themselves in the performance metrics. In other words, ***actual*** RSO motion is governed by the science of Astrodynamics. However, ***perceived*** RSO motion has contributions from Astrodynamics as well as information sources and modelling assumptions which include limitations in the models. The “Consider Covariance” implementation, described in the next section, addresses a method for accommodating modelling errors or so-called “known unknowns”. To address this, some additional tools have been proposed that apply state-of-the-art information theory. Such tools have been proposed for data-to-track and track-to-track association [11], and in this context, could be applied to determine which sources of epistemic uncertainty might be measurable and, hence, knowable and removable from the RSO state and parameter estimation and prediction process. Likewise, “Consider Covariance” has been a long-established method for assessing the effects of unmodeled observation and dynamic errors on the estimation and prediction performance [12].

5 Optical data collection and calibration

5.1 Errors in RSO Tracking and Processing

Errors in sensor data can be random, biased, and/or systematic [13], in other words both aleatory and epistemic, respectively. They can also be associated with the observation data, the modelling, the filtering, or the reference satellite ephemerides for calibration. The sensor hardware and all software in the astrometric processing chain can contribute to errors in each category as indicated in Figure 6. A representative categorization of these errors is as follows:

- Data
 - Astrometric errors
 - Random (Aleatory)
 - Systematic (Epistemic)
 - Reference frame of derived data
 - Timing bias
 - Aberration correction
 - Media delay corrections
 - Outliers
- Models
 - Dynamic mis-modeling errors
 - Observation modeling errors
- OD Filter (incorrect assumptions)
 - Initial state errors
 - Uncompensated biases
 - Incorrect noise assumed
 - Unmodeled dynamics (e.g. maneuvers)
 - Outliers not filtered
 - Mis-tags of data from mis-correlation (i.e. Type I and II errors)
- Calibration
 - Reference satellite error
 - Interpolation from tabular reference source (e.g. WAAS)
 - Initial state errors from osculating orbit source (e.g. TDRS)
 - Incorrect reference frame

5.2 The Calibration Process

Satellites with well-known orbits and accessible ephemeris data are used as calibration (“reference”) satellites, or “CalSats” for short. These orbital fiducials include (but may not be limited to) GNSS satellites such as GPS and Beidou, TDRS, and the Wide-Area Augmentation System (WAAS) constellations. Observations are correlated with specific CalSats for which their ephemeris data are collected, mapped into the observation reference frame, and interpolated to the observation timestamps. The calibration process involves computing the residuals between these reference data and the observation values reported. These residuals are then used to assess the quality and noise of the data, to validate that the correct reference frames and time-scales have been used, and to estimate any additional biases or systematic errors (i.e. this seeks to eliminate epistemic uncertainties). The optical calibration process identifies a “reference” satellite for which a highly accurate and precise ephemeris is available and tasks it to be tracked. The reference satellite orbit is reduced to derive a reference measurement set at the observation times which are compared to the actual measurements (e.g. topocentric right ascension and declination). The calibration process is depicted in Figure 7 where a suitably accurate reference satellite state may be established via a high accuracy OD process using tracking data from a previously vetted tracking network. As noted in the previous section, even the “calibrated” metrics can be subject to errors in the reference source (e.g. reference satellite state and reference frame conversion). Examples of “good” and “biased” calibration metric residuals are shown in Figures 8 and 9, respectively.

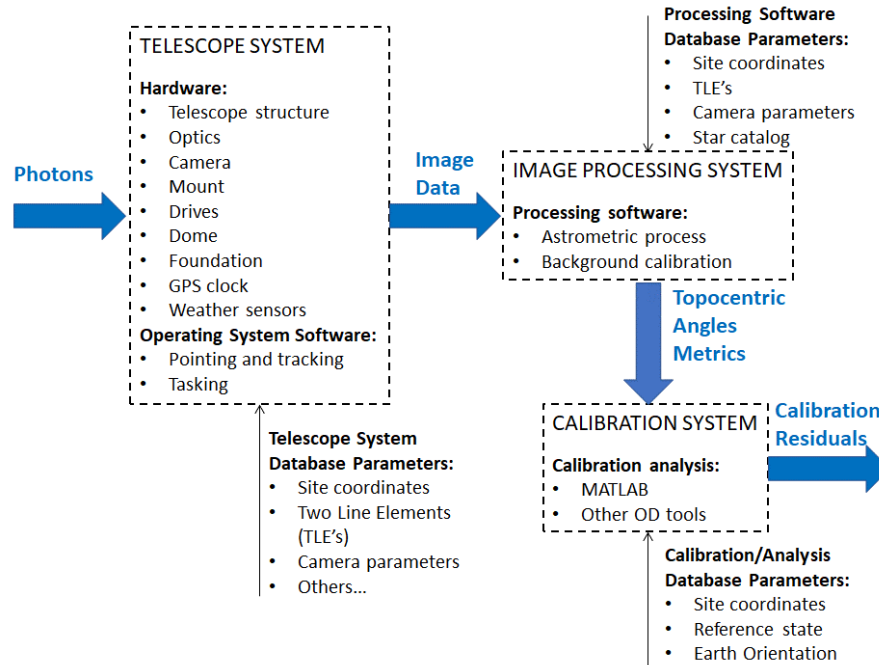


Figure 6 Sources of Astrometric Processing Error

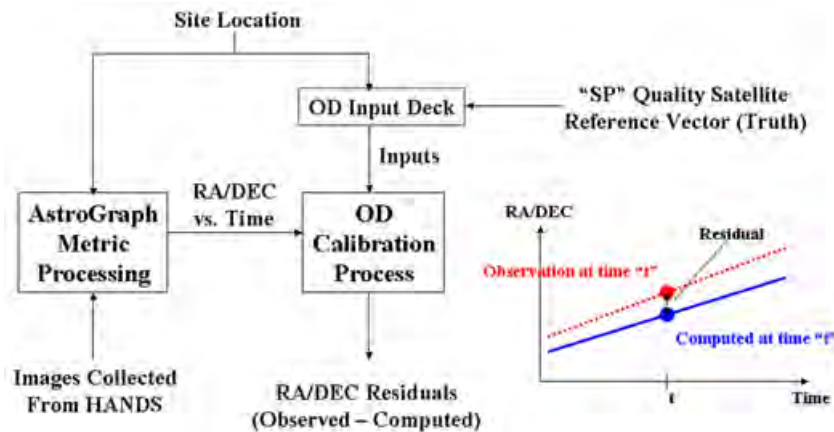


Figure 7. Optical Metric Calibration Process

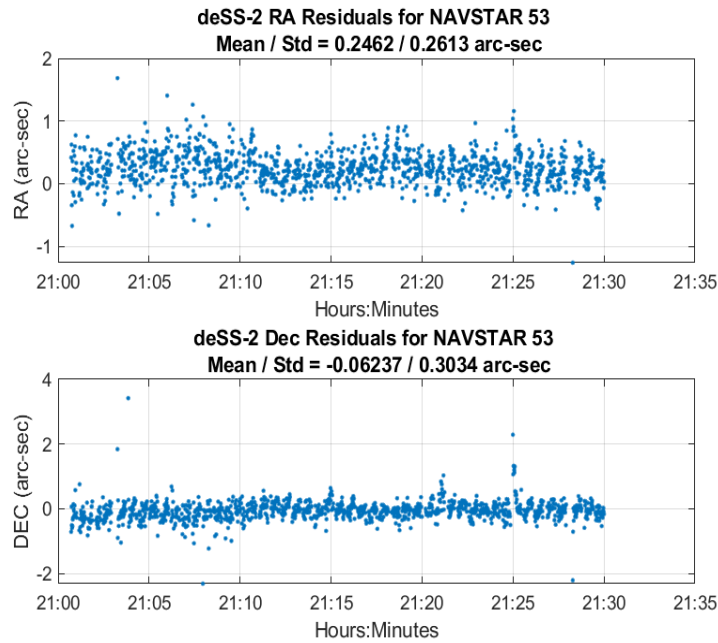


Figure 8. “Good” calibration example

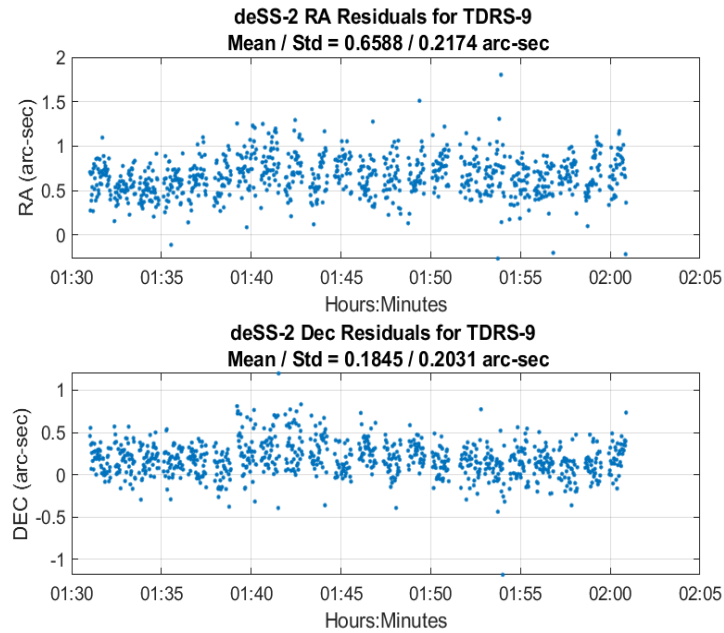


Figure 9. “Biased” calibration example

As noted in the *Introduction*, not all ground-based sensors will necessarily have visibility to an established reference satellite to perform sensor calibration. In this case, a reference can be “built” by fitting data from previously vetted sensors. The proposed filtering implementation presented in subsequent sections is intended for exactly this purpose.

5.3 DEIMOS Data Collection

A set of data were collected and “non-real-time” calibration results were generated to serve as a performance baseline from which the data integrity process can leverage *a priori* expectations for data performance and derived orbit products. The calibration metrics are used to develop data integrity methodologies, algorithms, and standards that can be used to reliably incorporate non-traditional data into established tracking networks in a timely fashion.

A set of reference satellites for which accurate orbits are known and available were tasked and tracked by the Deimos Tracker-2 optical telescope located in Southern Spain. The purpose was to obtain a set of EO data to use for the NRT dynamic calibration filter development and validation. A total of 14,925 observations whose noise statistics are assumed to be independent and identically distributed (i.i.d.) were collected and processed using the non-real-time process to pre-validate the measurements.

Table 2 shows the requested and actual executed taskings of the Deimos Tracker-2 sensor. The reported start and stop date/times (second column) versus the “tasked” start and stop date/times (first column) are shown for each satellite as specified by its international designator. A nominal 30-minute period of data were collected for each tasked satellite. Table 3 shows a summary of the raw observation files that were received after the night of tasking. In total, 20 files were received capturing 17 tracks of data, as tasked. The rows boxed in red highlight raw observation files that cover the same timespan for the same satellites.

Table 2. Task Planning

Requested	Executed
TLE 2018-05-20 20:00:00 14068A	TLE 2018-05-15 20:15:00 14068A
TLE 2018-05-20 20:30:00 14004A	TLE 2018-05-15 20:30:00 14004A
TLE 2018-05-20 21:00:00 03058A	TLE 2018-05-15 21:00:00 03058A
TLE 2018-05-20 21:30:00 02011A	TLE 2018-05-15 21:30:00 02011A
TLE 2018-05-20 22:00:00 04045A	TLE 2018-05-15 22:00:00 11036A
TLE 2018-05-20 22:30:00 08030A	TLE 2018-05-15 22:30:00 08030A
TLE 2018-05-20 23:00:00 04023A	TLE 2018-05-15 23:00:00 04023A
TLE 2018-05-20 23:30:00 07056B	TLE 2018-05-15 23:30:00 07056B
TLE 2018-05-21 00:00:00 14045A	TLE 2018-05-16 00:00:01 14045A
TLE 2018-05-21 00:30:00 14004A	TLE 2018-05-16 00:30:00 14004A
TLE 2018-05-21 01:00:00 03058A	TLE 2018-05-16 01:00:00 14026A
TLE 2018-05-21 01:30:00 02011A	TLE 2018-05-16 01:30:00 02011A
TLE 2018-05-21 02:00:00 04045A	TLE 2018-05-16 02:00:00 04045A
TLE 2018-05-21 02:30:00 08030A	TLE 2018-05-16 02:30:00 08030A
TLE 2018-05-21 03:00:00 04023A	TLE 2018-05-16 03:00:00 09043A
TLE 2018-05-21 03:30:00 07056B	TLE 2018-05-16 03:30:00 07056B
TLE 2018-05-21 04:00:00 14045A	TLE 2018-05-16 04:00:00 14045A
END 2018-05-21 04:30:00	END 2018-05-16 04:15:00

Table 3. Data Collection Summary

SensorID	COMMON_NAME	SSN	COSPAR	Nobs	Raw Files	START_TIME	STOP_TIME	DURATION INTERVAL	
								_MIN	_SEC
deSS-2	NAVSTAR 72	40294	14068A	561	1 of 1	5/15/2018 20:16	5/15/2018 20:30	14.24	1.52
deSS-2	TDRS-12	39504	14004A	1218	1 of 2	5/15/2018 20:30	5/15/2018 21:00	29.56	1.46
deSS-2	TDRS-12	39504	14004A	795	2 of 2	5/16/2018 00:31	5/16/2018 01:00	29.02	2.19
deSS-2	NAVSTAR 53	28129	03058A	1122	1 of 2	5/15/2018 21:00	5/15/2018 21:26	25.93	1.39
deSS-2	NAVSTAR 53	28129	03058A	135	2 of 2	5/15/2018 21:26	5/15/2018 21:30	3.13	1.39
deSS-2	TDRS-9	27389	02011A	1131	1 of 2	5/15/2018 21:31	5/15/2018 22:00	29.46	1.56
deSS-2	TDRS-9	27389	02011A	903	2 of 2	5/16/2018 01:31	5/16/2018 02:00	29.86	1.98
deSS-2	NAVSTAR 66	37753	11036A	1128	1 of 1	5/15/2018 22:02	5/15/2018 22:30	27.97	1.49
deSS-2	SKYNET 5C	33055	08030A	1155	1 of 4	5/15/2018 22:31	5/15/2018 23:01	29.91	1.55
deSS-2	SKYNET 5C	33055	08030A	111	2 of 4	5/15/2018 22:40	5/15/2018 23:01	20.87	11.28
deSS-2	SKYNET 5C	33055	08030A	927	3 of 4	5/16/2018 02:30	5/16/2018 03:01	30.39	1.97
deSS-2	SKYNET 5C	33055	08030A	360	4 of 4	5/16/2018 02:31	5/16/2018 03:01	29.69	4.95
deSS-2	NAVSTAR 55	28361	04023A	1068	1 of 1	5/15/2018 23:01	5/15/2018 23:30	28.94	1.63
deSS-2	SKYNET 5B	32294	07056B	1047	1 of 2	5/15/2018 23:31	5/16/2018 00:01	30.17	1.73
deSS-2	SKYNET 5B	32294	07056B	780	2 of 2	5/16/2018 03:31	5/16/2018 04:00	29.50	2.27
deSS-2	NAVSTAR 71	40105	14045A	1014	1 of 2	5/16/2018 00:01	5/16/2018 00:30	28.89	1.71
deSS-2	NAVSTAR 71	40105	14045A	138	2 of 2	5/16/2018 04:01	5/16/2018 04:08	6.80	2.96
deSS-2	NAVSTAR 70	39741	14026A	1038	1 of 1	5/16/2018 01:01	5/16/2018 01:30	29.36	1.70
deSS-2	NAVSTAR 56	28474	04045A	1023	1 of 1	5/16/2018 02:01	5/16/2018 02:30	28.59	1.68
deSS-2	NAVSTAR 64	35752	09043A	822	1 of 1	5/16/2018 03:02	5/16/2018 03:30	28.47	2.08

5.4 Non Real-time Calibration Results

Table 4 shows a summary of the calibration statistics for the EO observation data. Due to the low quality of TLE data, the SGP4 results for 32294 and 33055 should not be considered representative of the sensor’s true bias. All of the residuals with the exception of the SGP4 data and the first track of TDRS-9 data have sub-arcsecond biases and standard deviations. It is unclear why only 12 of the 1,131 observations for the first track of TDRS-12 data on 15 May were processed.

Table 4. Summary table of optical observations and calibration statistics

Track	Date Start (UTC)	Date End (UTC)	Object ID	Calsat Type	Duration (hours)	Number of Obs	RA bias (arcsec)	RA std (arcsec)	RA rss (arcsec)	Dec bias (arcsec)	Dec std (arcsec)	Dec rss (arcsec)
1	5/15/2018 21:31	5/15/2018 22:00	27389	TDRS	0.491	1131	2.583	0.259	2.596	0.234	0.183	0.297
2	5/15/2018 21:00	5/15/2018 21:30	28129	GPS	0.488	1257	0.246	0.261	0.359	-0.062	0.303	0.310
3	5/15/2018 23:01	5/15/2018 23:30	28361	GPS	0.482	1068	0.250	0.250	0.354	-0.092	0.293	0.307
4	5/15/2018 23:31	5/15/2018 23:58	32294	SGP4	0.465	1005	45.831	0.748	45.837	-47.742	1.291	47.760
5	5/15/2018 22:31	5/15/2018 23:01	33055	SGP4	0.498	1161	-3.570	0.316	3.584	1.417	0.406	1.474
6	5/15/2018 22:02	5/15/2018 22:30	37753	GPS	0.466	1128	0.197	0.249	0.318	-0.119	0.266	0.291
7	5/15/2018 21:00	5/15/2018 21:00	39504	TDRS	0.004	12	0.199	0.135	0.240	0.593	0.129	0.606
8	5/15/2018 20:16	5/15/2018 20:30	40294	GPS	0.237	561	0.170	0.289	0.335	0.239	0.330	0.407
9	5/16/2018 01:31	5/16/2018 02:00	27389	TDRS	0.498	903	0.659	0.217	0.694	0.185	0.203	0.274
10	5/16/2018 02:01	5/16/2018 02:30	28474	GPS	0.477	1023	0.172	0.330	0.372	0.056	0.265	0.270
11	5/16/2018 00:00	5/16/2018 04:00	32294	SGP4	4.011	822	44.296	2.871	44.389	5.406	2.331	5.887
12	5/16/2018 02:30	5/16/2018 03:01	33055	SGP4	0.509	1047	9.899	0.710	9.924	-4.999	0.320	5.009
13	5/16/2018 03:02	5/16/2018 03:30	35752	GPS	0.475	822	0.098	0.368	0.381	0.085	0.334	0.344
14	5/16/2018 00:31	5/16/2018 01:00	39504	TDRS	0.484	795	0.278	0.344	0.443	-0.063	0.320	0.326
15	5/16/2018 01:01	5/16/2018 01:30	39741	GPS	0.489	1038	0.322	0.383	0.500	-0.120	0.317	0.339
16 & 17	5/16/2018 00:01	5/16/2018 04:08	40105	GPS	4.110	1152	0.445	0.507	0.675	-0.163	0.470	0.498

With the exception of a few cases where the data collections occurred during calibration satellite manoeuvres, the right ascension and declination measurements were less than a half of an arc-second³. These data collected on a combination satellites in medium and Geosynchronous Earth orbits (MEO and GEO) will be more than adequate to support the dynamic calibration development and assessment. Though we retain the option of collecting additional data to support follow-up dynamic calibration demonstrations, the data collected for this assessment are of more than adequate quality to support the current development. These data are to be used to validate the dynamic calibration and data integrity processes. The analysis results should be most helpful in guiding requirements for any subsequent data collection campaigns.

³ 1 arc-second at GEO from the Earth’s surface is roughly an arclength equivalent to 175 meters.

6 Unscented Schmidt Kalman Filter formulation

6.1 USKF Background

The proposed data integrity processes, to be exercised in NRT, require an estimation implementation that enables certain parameters to be estimated and others only to be considered during the estimation process, e.g. observation biases, until the appropriate reference satellite data are available. This section outlines that approach.

In order to account for, or “consider”, the uncertainty associated with non-estimated parameters, the Unscented Schmidt-Kalman filter (USKF) is utilized. It incorporates the “consider covariance analysis” concept whereby known errors in model and state parameters can be “considered” to make the estimation uncertainty more representative (realistic). As previously stated, this allows a user to account for so-called *known unknowns*. Using by-products of the USKF algorithm, the Fisher information can be computed, giving a measure of the observability of estimated parameters.

Stauch and Jah [14] presented the USKF which is well suited to this application. There are two general categories of consider techniques. One is consider analysis, in which a typical state filter is executed and after the measurement update, the uncertainties of the consider parameters are mapped into the state space. The other is a consider filter, in which the state itself is augmented with the consider parameters while the consider parameter value and uncertainty are forced to be unchanged. Thus, the consider parameters are directly included in the filtering process. The USKF algorithm used in this work is given in Table 5.

Note that $X_{i,k}$ and P_k are the state and covariance of the estimated parameters only, $Z_{i,k}$ and $P_{zz,k}$ are the augmented state and covariance (i.e. both estimated and considered parameters). Notice that the key difference between the filters is that the update to the consider state and covariance terms are forced to be zero, while the consider-estimated parameter cross-covariance term updates are maintained. This makes the USKF a sub-optimal filter but one that is useful in preventing a falsely optimistic estimate. This is sometimes referred to as “covariance realism.” Parameters such as measurement related biases can be considered until reference satellite data are available.

Table 5. USKF Formulation

USKF
<u>Predictive</u>
$\mathbf{S}_{zz,k-1} = \text{Cholesky}(\mathbf{P}_{zz,k-1})$ $\mathbf{Z}_{i,k-1} = \hat{\mathbf{z}}_{k-1} \pm \sqrt{n_x + n_c} \mathbf{s}_{i,k-1}$ <p style="margin-left: 40px;">where $\mathbf{S}_{zz} = [\mathbf{s}_1, \dots, \mathbf{s}_{n_x+n_c}]$</p> $w = \frac{1}{2^{(n_x+n_c)}}$ $\mathbf{Z}_{i,k} \leftarrow \dot{\mathbf{Z}}_i = \mathbf{f}(\mathbf{Z}_{i,k-1}, t)$ $\hat{\mathbf{z}}_k = \sum_{i=1}^{2^{(n_x+n_c)}} w_i \mathbf{Z}_{i,k}$ $\mathbf{P}_{zz,k} = \sum_{i=1}^{2^{(n_x+n_c)}} w_i (\mathbf{Z}_{i,k} - \hat{\mathbf{z}}_k)(\mathbf{Z}_{i,k} - \hat{\mathbf{z}}_k)^T$
<u>Corrective</u>
$\mathbf{Y}_i = \mathbf{h}(\mathbf{Z}_i, t)$ $\hat{\mathbf{y}} = \sum_{i=1}^{2^{(n_x+n_c)}} w_i \mathbf{Y}_i$ $\mathbf{P}_{yy} = \sum_{i=1}^{2^{(n_x+n_c)}} w_i (\mathbf{Y}_i - \hat{\mathbf{y}})(\mathbf{Y}_i - \hat{\mathbf{y}})^T + \mathbf{R}$ $\mathbf{P}_{zy} = \sum_{i=1}^{2^{(n_x+n_c)}} w_i (\mathbf{Z}_i - \hat{\mathbf{z}})(\mathbf{Y}_i - \hat{\mathbf{y}})^T$ $\begin{bmatrix} \mathbf{P}_{xy} \\ \mathbf{P}_{cy} \end{bmatrix} = \mathbf{P}_{zy}$ $\mathbf{K}_z = \mathbf{P}_{zy} \mathbf{P}_{yy}^{-1} = \begin{bmatrix} \mathbf{K}_x \\ \mathbf{K}_c \end{bmatrix} \quad (\text{NOTE: } \mathbf{K}_c \neq 0!!)$ <p style="margin-left: 40px;">Force correction to consider terms to be 0:</p> $\hat{\mathbf{z}}^+ = \hat{\mathbf{z}}^- + \begin{bmatrix} \mathbf{K}_x \\ \mathbf{0} \end{bmatrix} (\mathbf{y} - \hat{\mathbf{y}})$ $\mathbf{P}_{zz}^+ = \begin{bmatrix} \mathbf{P}_{xx}^- & \mathbf{P}_{xc}^- \\ \mathbf{P}_{cx}^- & \mathbf{P}_{cc}^- \end{bmatrix} - \begin{bmatrix} \mathbf{K}_x \mathbf{P}_{yy} \mathbf{K}_x^T & \mathbf{K}_x \mathbf{P}_{yy} \mathbf{K}_c^T \\ \mathbf{K}_c \mathbf{P}_{yy} \mathbf{K}_x^T & \mathbf{0} \end{bmatrix}$

6.2 Consider Parameter Implementation

Parameters in an estimator can either be ignored, considered or estimated (referred to as “ice”). In this application the state consists of satellite position, velocity, solar radiation pressure and sensor related biases (e.g. *time-tag bias*). In some instances, some of these filter parameters may not be “observable,” i.e., there is insufficient information in the observations to estimate them. In this case we might “consider” the parameter – that is, account for our knowledge of its uncertainty in the filter estimates and covariance without estimating it.

6.3 Use of Fisher Information

The observation information content regarding the sensor bias is explored to develop a method that detects its observability and thus determine when it can be inferred from the available data. Likewise, other parameters associated with the estimation of RSO and sensor characteristics may or may not be observable. This knowledge can be used to determine when one might decide when to “consider” a parameter based on the availability of reference satellite data. Likewise, once a parameter becomes observable, this knowledge can be used to switch a parameter from being considered to estimated. We propose the use of the Fisher Information matrix. The pseudo Fisher information in the USKF is computed given the pre-update state covariance, \bar{P} , the measurement noise matrix R and the state vs. the observation cross covariance P_{xy}

$$F_{info} \approx \tilde{H}^T R^{-1} \tilde{H} \quad (1)$$

where

$$\tilde{H} = (\bar{P}^{-1} P_{xy})^T \quad (2)$$

This metric can be viewed as a measure of the state information content provided in the observation data [15, 16, 17]. More specifically, it quantifies how changes in the measurements result in changes to the state. Information content is always higher with greater differences or rates of change.

6.4 Estimated vs. Consider State Implementation

The EO data require that the reference orbit information be available in order to estimate sensor-related biases. The process initializes the filter by including the reference orbit information in the state at a point in time just prior to the first EO data time-tag. At the point where EO data and the reference information are both available, the sensor bias can then be estimated until that parameter is sufficiently converged. At that point, the EO data should be monitored for consistency over a specified time span before it can be completely trusted. In other words, does the hypothesized bias achieve some steady state in the presence of increasing evidence? This process is illustrated in Figure 10.

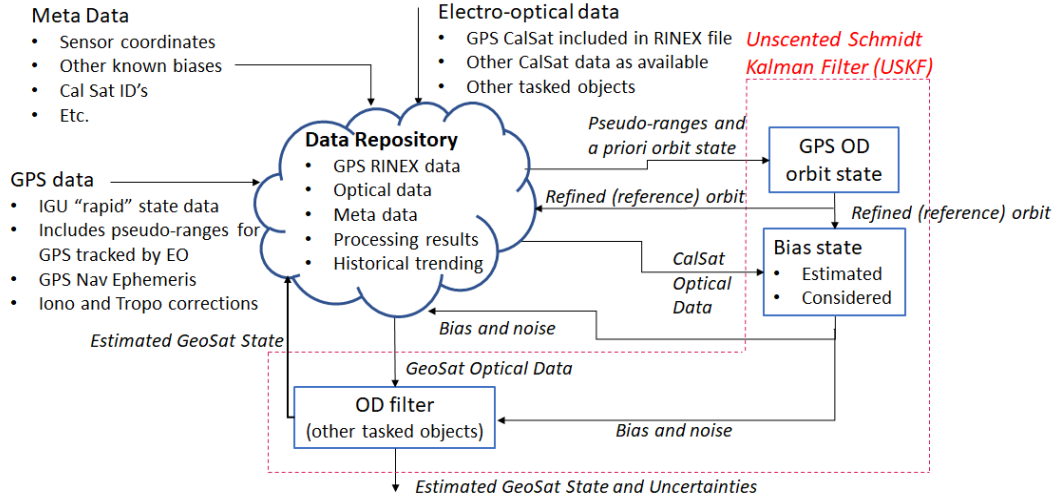


Figure 10. Estimation and Consider Process

6.5 USKF Time Bias Formulation

Though, in general, all forms of error (e.g. biases, systematic and periodic errors) are of interest, the subsequent use-cases model a sensor timing bias to illustrate the near real-time calibration using the USKF. Hence, in order to either estimate or consider the timing bias, it must be included in the USKF state along with any other estimated parameters (e.g. *position, velocity and solar radiation pressure*). The timing bias finds its way into the USKF via the EO reference measurements derived from the reference satellite. The reference satellite is tracked by the EO sensor and the EO sensor inertial state (derived from the site coordinates) at the measurement time is corrected for the timing bias. At the time of each measurement update the state-vector sigma points are used to compute an equivalent measurement sigma point and these are adjusted for the current best estimate of the timing bias as follows

$$t_{corrected} = t_{observation} - t_{bias} \quad (3)$$

$$\vec{R}_{J2000} = [T_{ITRF \rightarrow J2000}(t_{corrected})] \vec{R}_{ITRF} \quad (4)$$

$$\vec{\rho} = \vec{r}_{J2000} - \vec{R}_{J2000} - \vec{v}_{J2000} \cdot (t_{bias} + \delta t_{LTC}) \quad (5)$$

$$\rho = \|\vec{\rho}\| = \sqrt{\rho_x^2 + \rho_y^2 + \rho_z^2} \quad (6)$$

$$\alpha = \tan^{-1} \left(\frac{\rho_y}{\rho_x} \right) \quad (7)$$

$$\delta = \sin^{-1} \left(\frac{\rho_z}{\rho} \right) \quad (8)$$

where R_{J2000} is the sensor inertial position; r_{J2000} and v_{J2000} are the satellite inertial position and velocity; ρ is the range vector between the sensor and satellite; α and δ are the “computed” optical measurements right ascension and declination; and δt_{LTC} is the light travel time correction that is applied to the optical measurements.

7 Dynamic calibration results

7.1 Analysis Background

An overview of the two-satellite two-sensor scenario is presented in Figure 11 and illustrates, for two satellites and two EO sensors, how the filter would leverage common observations to enhance information needed to estimate biases and assess performance. An outline of the process to be implemented is as follows:

1. Collect EO data (Optical 1) on a designated GPS (GPS 1) “reference” satellite.
2. Acquire the reference GPS satellite data from an International GNSS Ultra-rapid (IGU) file.
3. Refine the orbit of the tracked GPS (GPS 1) using IGU data (including SRP).
4. Estimate sensor noise and biases for the EO sensor (Optical 1) using the EO data and the refined reference satellite state.
5. Use the EO site with updated biases (Optical 1) to track a satellite in common (GeoSat) with another optical site (Optical 2)
6. Use GeoSat data as “reference for calibrating from Optical 2 sensor.
7. Continue to develop a network of vetted sensors using a multi-state filter which incorporates assessment of data and states to determine data integrity of newly included EO sensors and monitor existing sensors.

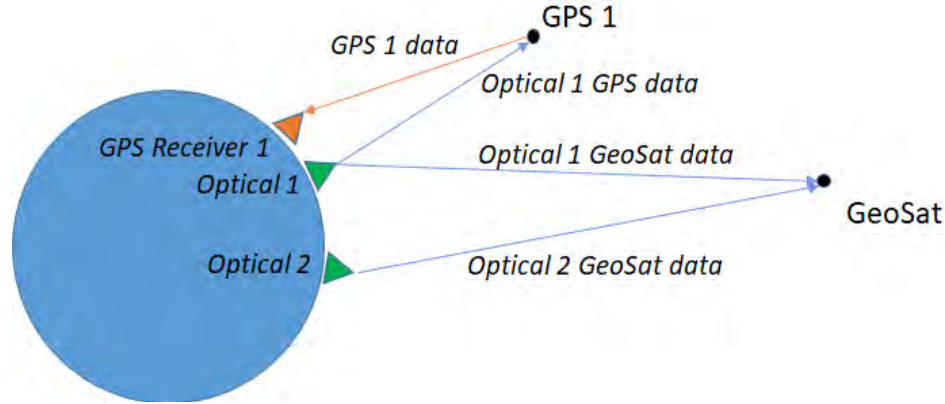


Figure 11. 2-satellite / 2-sensor Use Case Scenario

7.2 Two-Satellites and Two-Sensors Simulation Results

A two-satellite, two-sensor use case was simulated which included both reference data and EO tracking of a GPS reference satellite (GPS-PRN03) from a sensor located in Southern Spain, and a second GEO satellite (TDRS-9) tracked by an EO sensor located in South Africa. The tracking “Access” times are shown in Figure 12. In this use case example GPS-PRN03 is the “Reference” and TDRS-9 is the “RSO.”

The USKF state consisted of two sets of satellite states, one for the reference, X_{ref} , and one for the GEO RSO, X_{rso} ,

$$\vec{X} = \begin{bmatrix} \vec{X}_{ref} \\ \vec{X}_{rso} \\ \delta \vec{t} \end{bmatrix} \quad (9)$$

where the reference state is

$$\vec{X}_{ref} = \begin{bmatrix} \vec{r}_{ref} \\ \vec{v}_{ref} \\ \gamma_{ref} \end{bmatrix} \quad (10)$$

the RSO state is

$$\vec{X}_{rso} = \begin{bmatrix} \vec{r}_{rso} \\ \vec{v}_{rso} \\ \gamma_{rso} \end{bmatrix} \quad (11)$$

the optical sensor bias state is

$$\delta \vec{t} = \begin{bmatrix} \delta t_1 \\ \delta t_2 \end{bmatrix} \quad (12)$$

The two optical sensor biases assumed to be timing (other biases can be included in the state and estimated as appropriate) are δt_1 and δt_2 . The position and velocity cartesian vectors for the reference and RSO are

$$\vec{r} = \begin{bmatrix} r_x \\ r_y \\ r_z \end{bmatrix} \quad (13)$$

$$\vec{v} = \begin{bmatrix} v_x \\ v_y \\ v_z \end{bmatrix} \quad (14)$$

and the relevant solar radiation pressure term for each is defined as

$$\gamma = C_r \frac{A}{m} \quad (15)$$

where C_r is the radiation pressure coefficient, A is the effective cross-sectional area and m is the mass.

The 2-satellite and 2-optical sensor use case have both EO sensors tracking a common GEO satellite ("RSO") and one of the EO sensors also tracking a GPS ("Reference") for which it has accurate IGU states. The EO sensor tracking the GPS is located in Southern Spain while the second EO sensor is located in South Africa. Both satellite position and velocity states, and each of the time biases converge. The SRP term for the GPS reference converges but the SRP term for the RSO (GEO) satellite evidently needs more than a few hours of data. The "Access" for this tracking scenario is shown in Figure 12.

The EO sensors were modelled to have a noise value of 0.5 arc-seconds, 1- σ , per right ascension and declination component, whereas each of the GPS IGU state components were generated with a 1- σ noise of 5 cm. The EO measurements were generated at a 60 second sample interval and the GPS state measurements at a 15-minute interval, consistent with the IGU files. Initial position errors of several kilometres, and velocity errors of meters-per-second, were also included in the initial satellite states. SRP errors for each satellite, and timing biases of 250 milliseconds and 350 milliseconds for the Spain and South Africa optical sensors, respectively, were used.

The estimate of the reference satellite position and velocity state errors are shown in Figures 13 and 14, respectively, and are seen to be predominately influenced by the more accurate IGU measurements. Similarly, the position and velocity state errors for the RSO are provided in in Figures 15 and 16 and are initially larger and converge to 100's of meters based on the EO measurements.

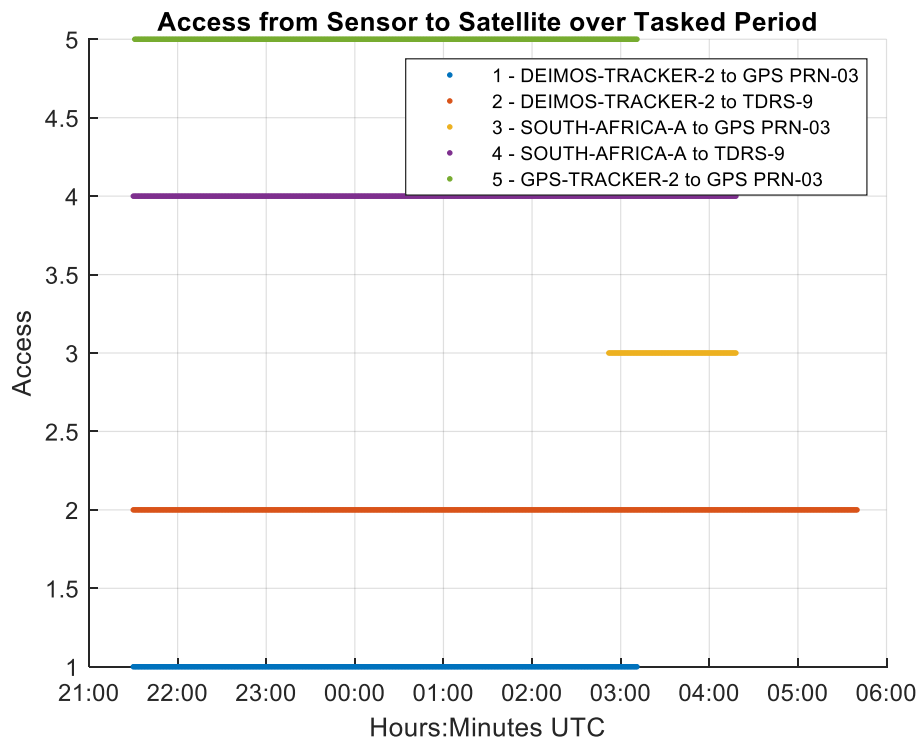


Figure 12. Access for 2-satellite / 2-sensor use case

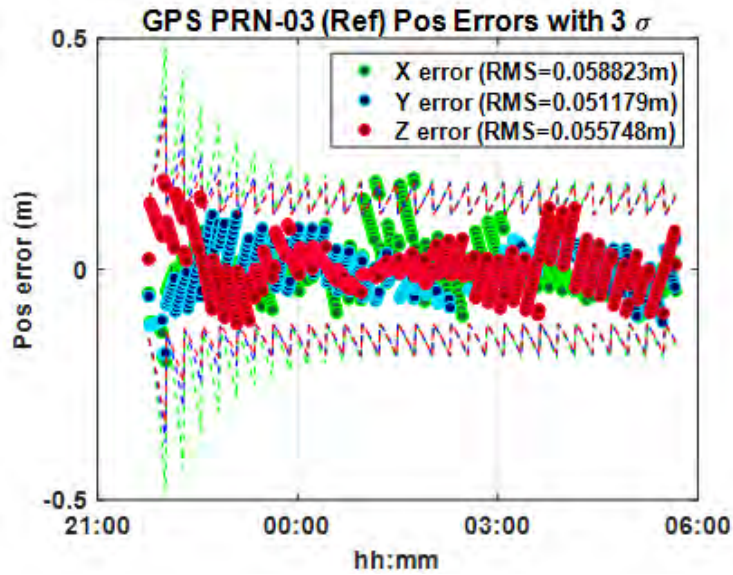


Figure 13. Reference orbit position estimate error and 3- σ uncertainty

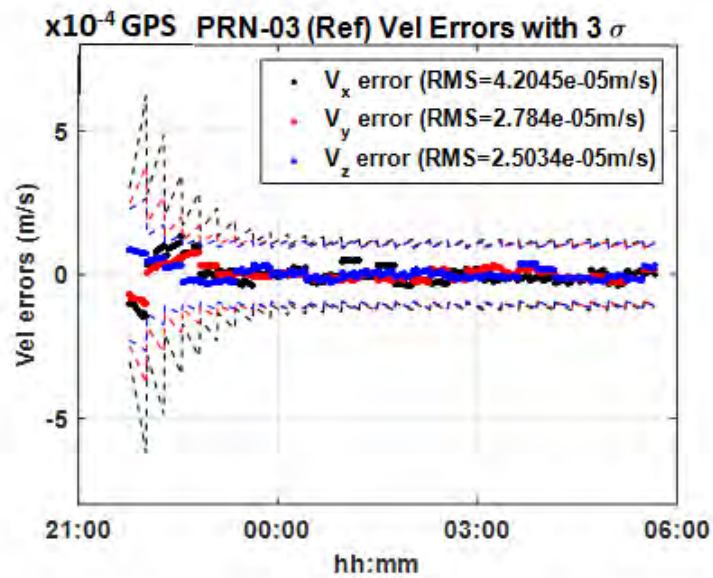


Figure 14. Reference orbit velocity estimate error and 3- σ uncertainty

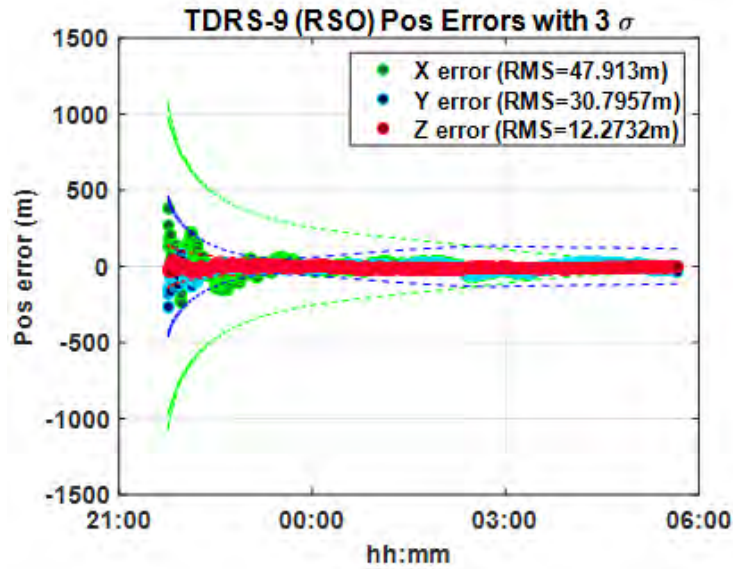


Figure 15. RSO orbit position estimate error and 3- σ uncertainty

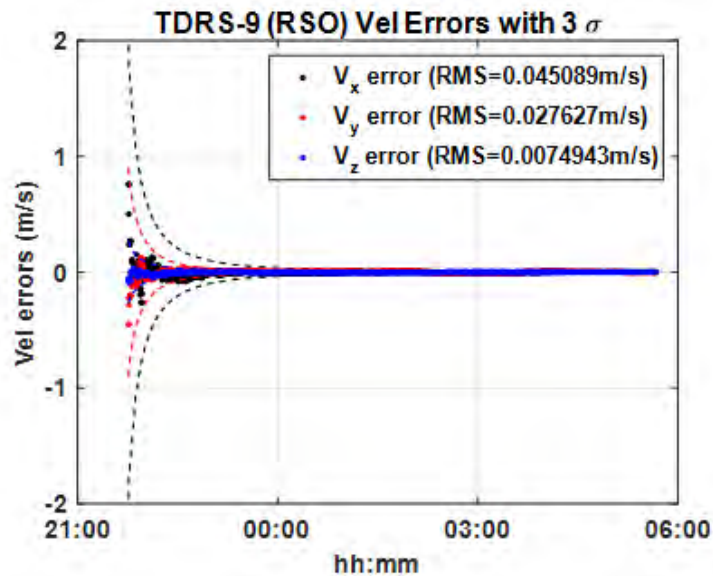


Figure 16. RSO orbit velocity estimate error and 3- σ

The SRP estimation errors are given in Figure 17 and indicate that the SRP for the reference satellite converges within an hour, again, due to the highly accurate IGU state measurements. The RSO SRP is much slower to converge, even after several hours, but perhaps is expected for the GEO EO tracking and geometry.

The simulated timing bias estimation errors for Sensor #1 and Sensor #2 are shown in Figure 18. The Sensor #1 bias, estimated using the reference state, converges after 1-2 hours whereas the Sensor 2 bias which relies on convergence of the RSO takes an additional 2-3 hours to converge. Additional studies will be conducted to evaluate the Concept of Operations (CONOPS) that best utilizes both the reference and EO data in the combined state filter. Additional implementation of some of the estimated parameters as consider parameters will also be explored to see if this expedites convergence.

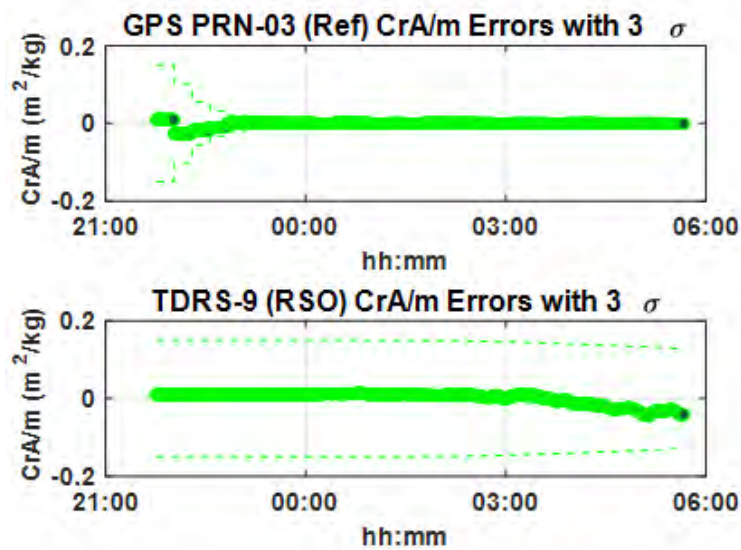


Figure 17. Reference orbit and RSO SRP errors and 3- σ uncertainty

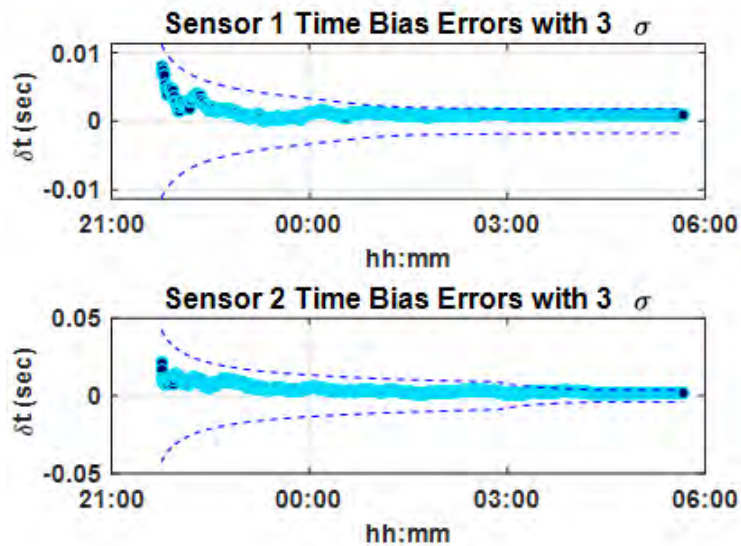


Figure 18. Optical sensor #1 and sensor #2 timing bias estimation error and 3- σ uncertainty

7.3 Real Data Single-Satellite and Single-Sensor

The single satellite and sensor state are similarly defined and implemented as in § 5.2 for a single satellite and single sensor where actual data for a GPS reference and EO data from the DEIMOS tracker were processed. An artificial time bias of 250 milliseconds was injected into the time tags of the EO measurements and processed in the USKF where the IGU GPS states were used as the reference source. The position, velocity and time bias estimates (SRP was considered) and the position error versus the known truth International GNSS Rapid (IGR) orbit data shown in Figure 19. The reference state was incorporated into the filter and when the EO data became available around 21:00h the time bias was estimated and converged almost immediately to within 1 millisecond of the known truth of 250 milliseconds as shown in Figure 20. The pre-fit residuals are shown in Figure 21 for the case where the observation timing bias is included but not estimated (upper) and for when the bias is estimated (lower). This illustrates the utility of using pre-fit residuals to detect biases. The IGU reference orbit position states relative to the IGR orbit is shown in Figure 22 and can be seen to be accurate to the centimetre level. Further exercising of the actual data using multiple reference and RSO satellites will be examined in future work.

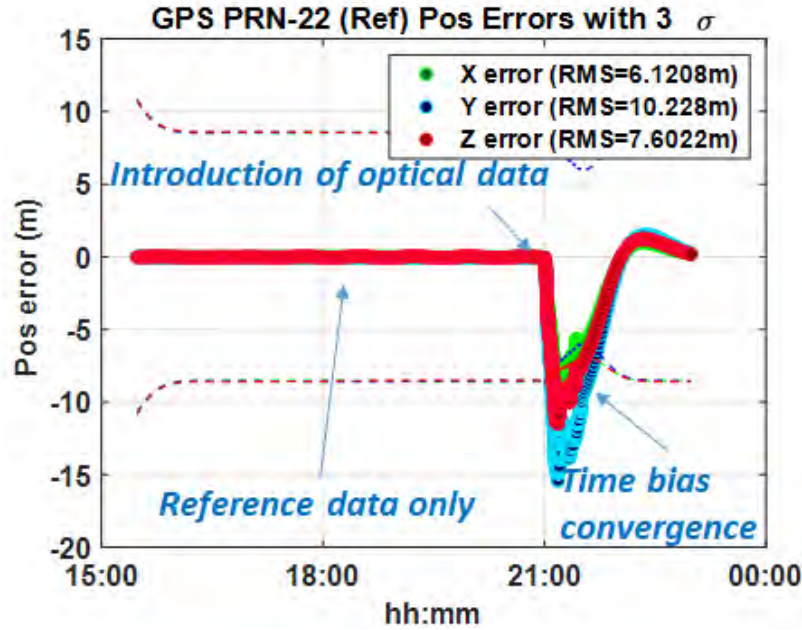


Figure 19. Reference orbit position estimate error and 3- σ uncertainty

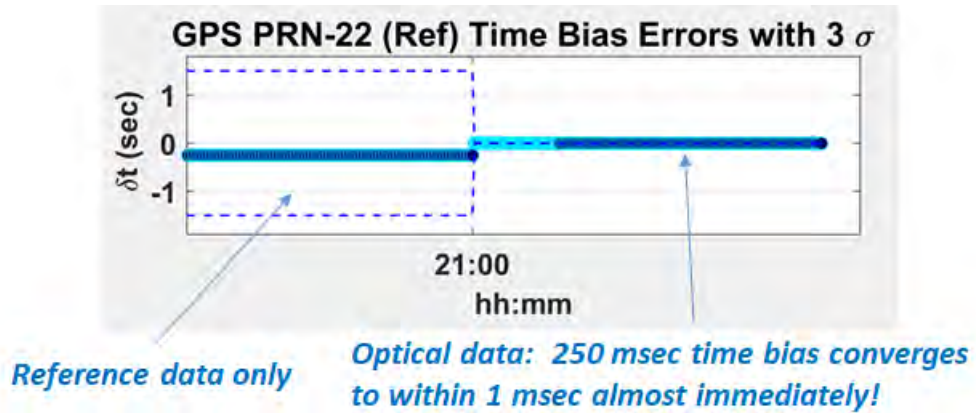


Figure 20. Time bias estimation error

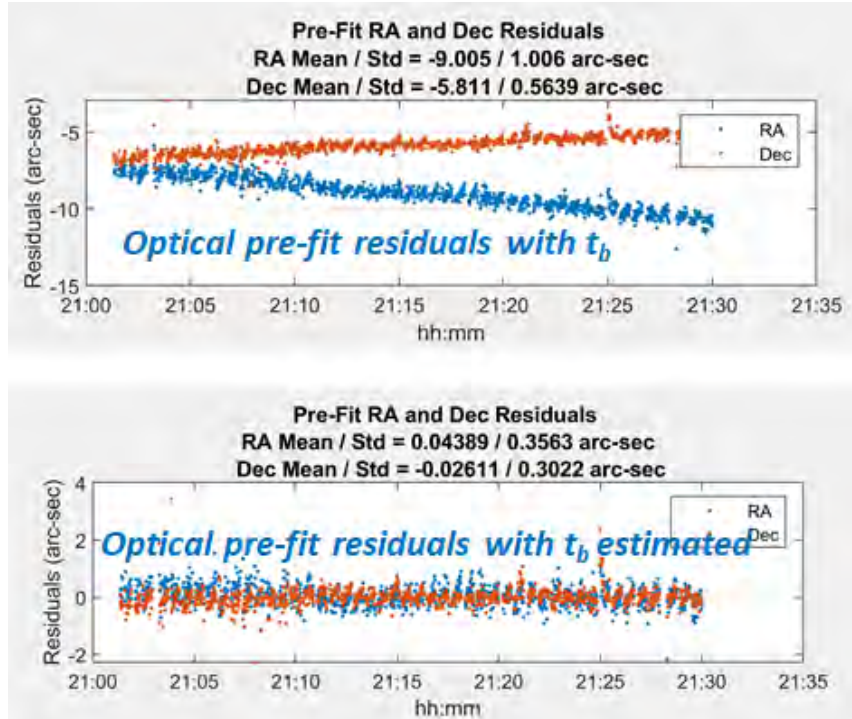


Figure 21. Pre-fit optical data (RA/Dec) residuals when time bias is included but not estimated (upper) and when time bias is estimated (lower)

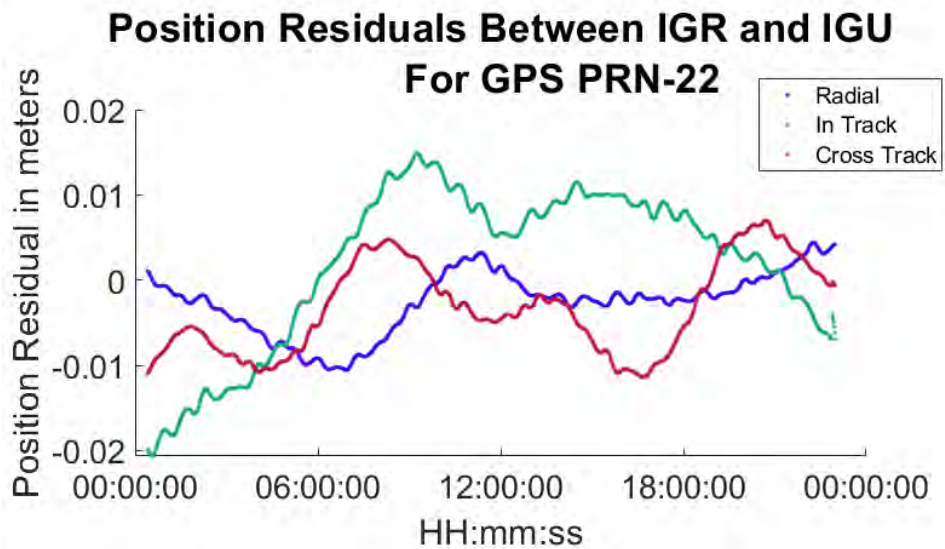


Figure 22. IGU reference orbit x, y, z position error relative to IGR reference states

8 Dynamic calibration analysis results for multiple satellites and sensors

8.1 Analysis Scenario Background

The 8-satellite and 2-optical sensor use case has both EO sensors tracking a common set of GEO satellites ("RSOs") and one of the EO sensors also tracking a GPS ("Reference") for which it has accurate IGU states. The EO sensor tracking the GPS is located in Southern Spain while the second EO sensor is located in South Africa. Both satellite position and velocity states and each of the sensor time biases converge. The SRP term for the GPS reference converges but the SRP term for the RSO (GEO) satellite evidently needs more than a few hours of data. The tracking geometry for the 8-satellite, 2-sensor scenario is shown in Figure 23 while the "Tracking Access" for this scenario is shown in Figure 24. The 8 satellites consist of 7 satellites in GEO orbits and one GPS "reference satellite" in a medium Earth orbit (MEO). The EO observations were simulated for all objects, though only the Southern Spain sensor tracked the GPS reference. The IGU (International GNSS Ultra-rapid Orbit Services) reference state data were also simulated for the GPS reference satellite.

The EO sensors were modelled to have a noise value of 0.5 arc-seconds, 1- σ , per right ascension and declination component, whereas each of the IGU state components for the GPS reference satellite were generated with a 1- σ noise of 5 cm. The EO measurements were generated at a 60-second sample interval and the GPS state measurements at a 15-minute interval, consistent with the IGU files. Initial position errors of several kilometres and velocity errors of meters-per-second were also included in the initial satellite states. SRP errors of 10% for each satellite and timing biases of 250 milliseconds for each of the Spain and South Africa optical sensors were used.

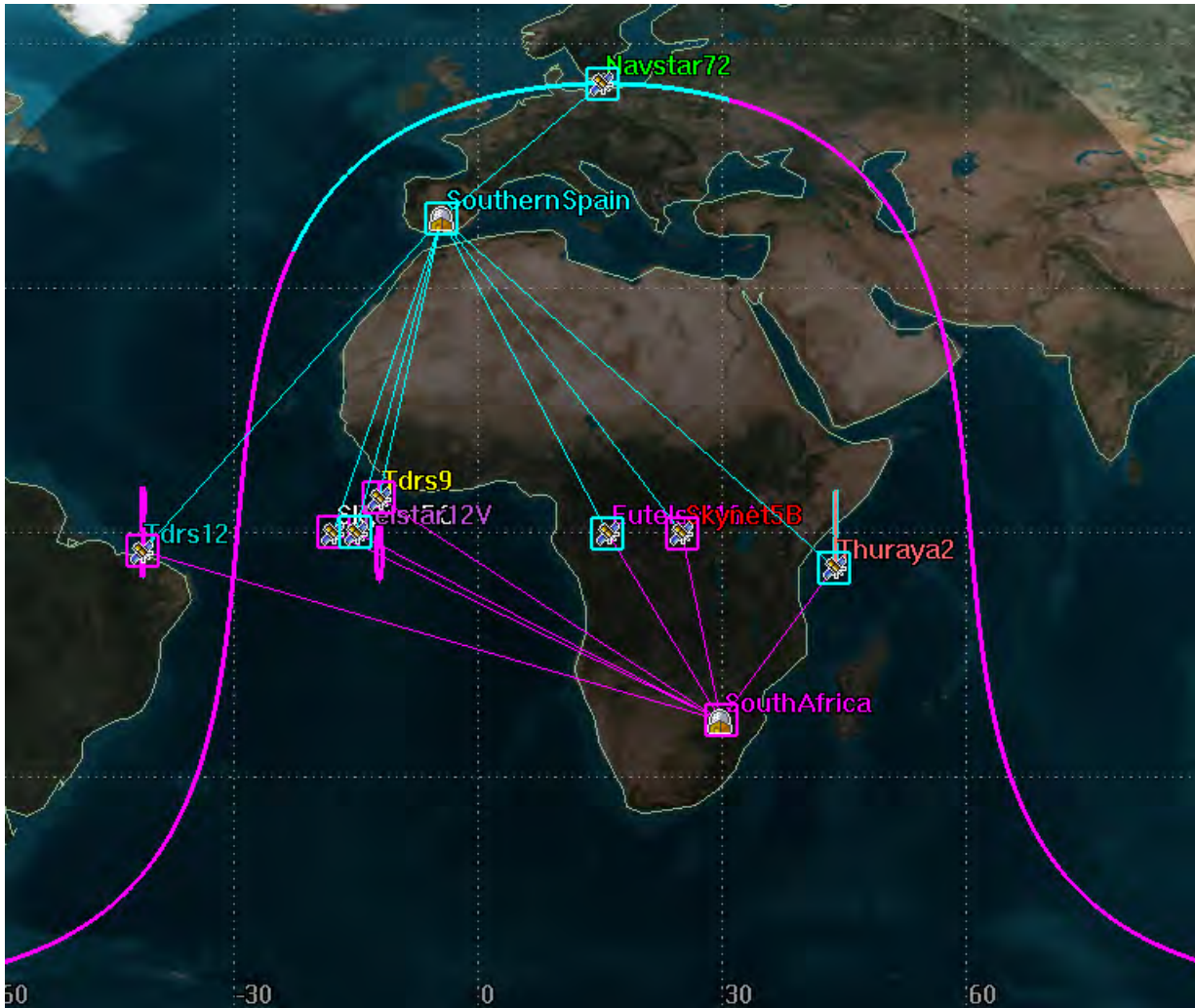


Figure 23. Tracking Geometry for 8-satellite / 2-sensor use case

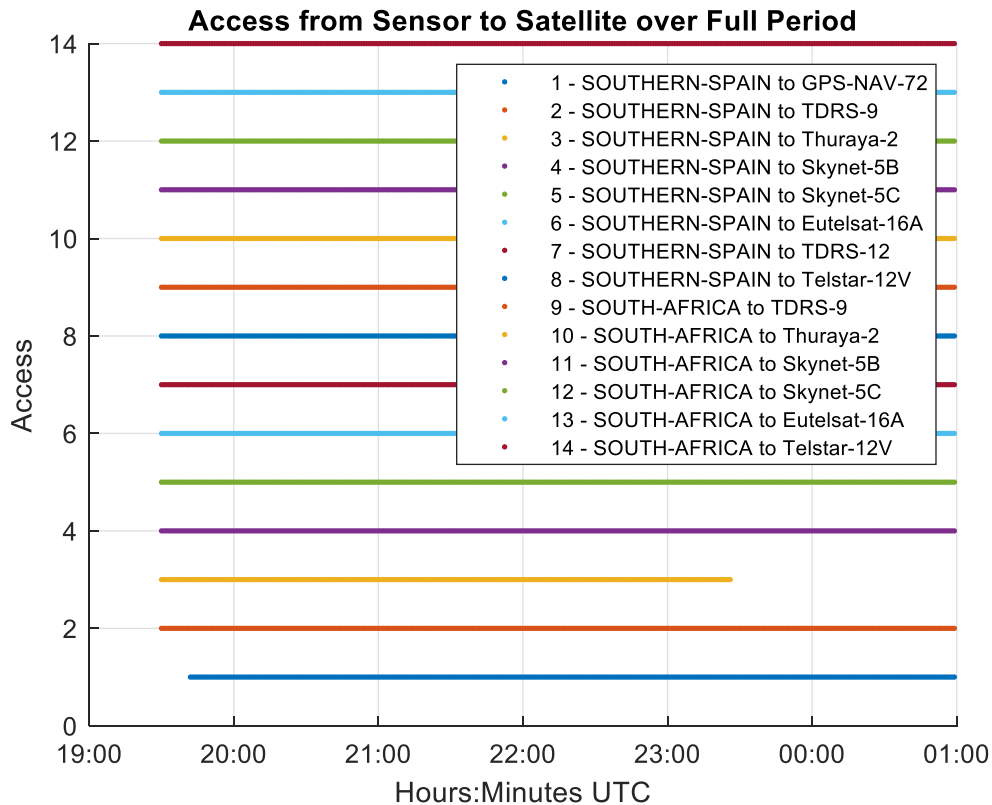


Figure 24. Tracking Access for 8-satellite / 2-sensor use case

8.2 Analysis Results for when Reference Satellite is Included in the Filter

The implementation requires that at least one of the EO sensors track a “reference satellite” for which an accurate reference ephemeris is available. In this example the reference is GPS-NAV-72 and the IGU states, which is available in near real-time, are used as “pseudo-observations” to update the state in the filter. The simultaneous tracking by the EO sensor, Southern Spain in this case, enables the time bias for that sensor to be directly estimated. While the IGU states only include the Cartesian positions, use of them in the filter as observations will enable estimates of the velocity and SRP parameter to insure accurate predictions in the multi-state filter to support accurate EO time bias calibration.

For the use case spanning 5+ hours (Figure 24) the estimate of the reference satellite position, velocity and SRP state errors are shown in Figures 25, 26 and 27, respectively, and are seen to be

predominately influenced by the more accurate IGU measurements with converged position accuracies vs. the known “truth” data on the order of meters. The pre- and post-fit residuals for the position measurements, provided in Figure 28, are seen to be on the order of meters which is in line with previously documented accuracies for the IGU states^{4, 10}.

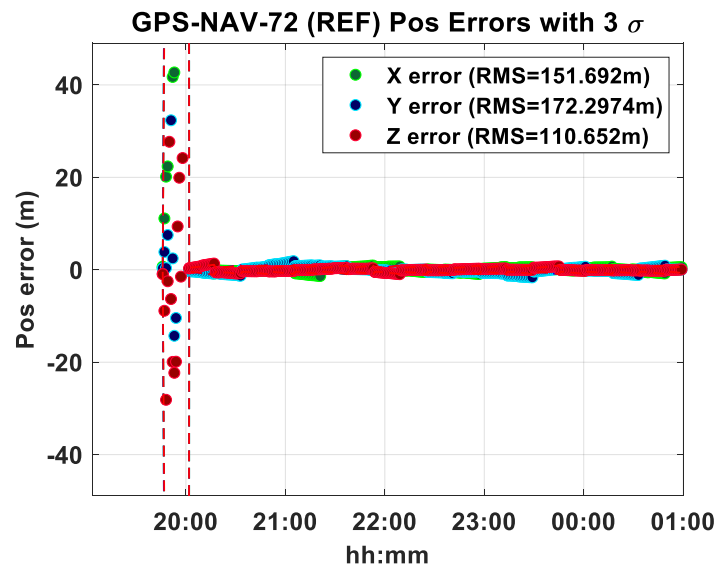


Figure 25. GPS Reference orbit position estimate error and 3- σ uncertainty

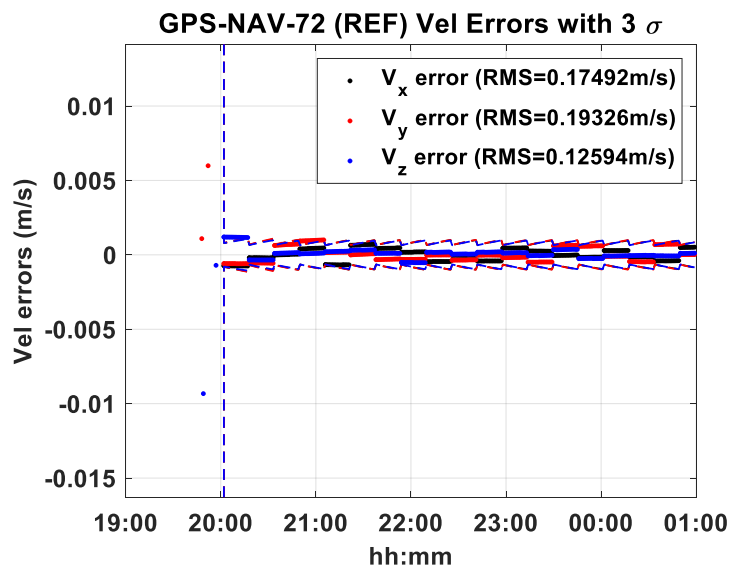


Figure 26. GPS Reference orbit velocity estimate error and 3- σ uncertainty

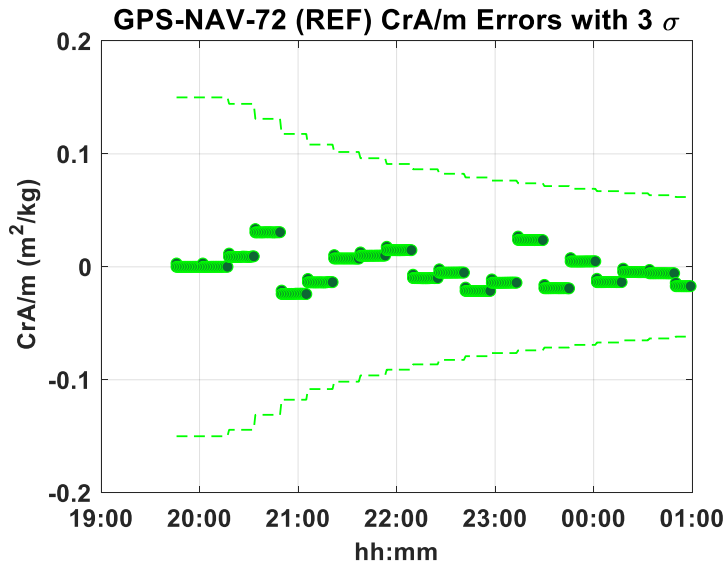


Figure 27. GPS Reference orbit SRP estimate error and 3- σ uncertainty

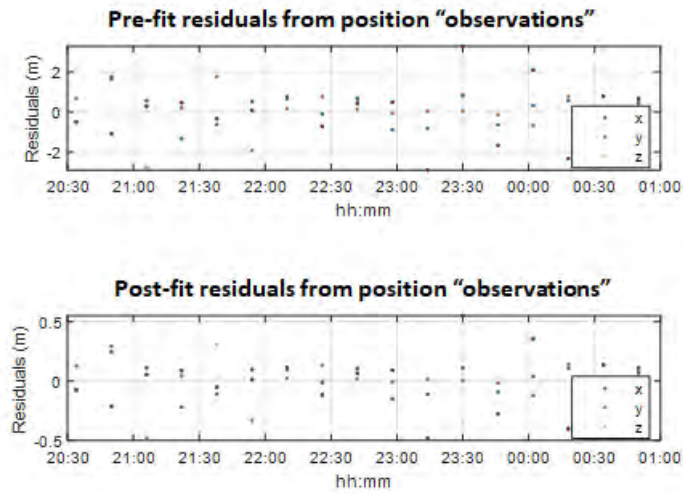


Figure 28. GPS Reference orbit position observation residuals

A summary of the dynamic filter results is provided in Table 6 for the 8 satellite states. The root sum squared (RSS) of the position, velocity and SRP estimates are provided for the case where the time bias was estimated and for where it was considered. In most cases the RSO position and velocity errors get worse for the consider case, but not terribly worse, the reason likely being a combination of

the sensor timing biases being considered and the influence (via the covariance correlations) of the GPS reference satellite state derived from the highly accurate IGU position measurements. One exception is noted for the Telstar-12V state which is marginally worse which is believed to be due to a slower convergence time. This will be further examined to confirm the reason. Note, also, the GPS reference is significantly worse when time biases are considered, a consequence of degradation due to biased EO measurements in the GPS reference state solution. Finally, the measurement time spans only 4-5 hours which is typically inadequate for estimating the SRP which usually requires data spanning 3 or more days for typical operational satellite area-to-mass ratios ($\sim 0.03 \text{ m}^2/\text{kg}$). The SRP estimates are provided though they did not converge over the time span of the analysis.

Table 6. Summary of estimated vs. consider from multi-state dynamic filter: Accurate IGU state included in the USKF updates

Sat Name	SSN i.d.	Type	Time Bias Estimated			Time Bias Considered		
			Pos Rss (m)	Vel Rss (m/s)	CrA/m Rss (m^2/kg)	Pos Rss (m)	Vel Rss (m/s)	CrA/m Rss (m^2/kg)
TDRS-9	27389	RSO	192.599	0.418	1.341E-03	204.167	0.436	5.551E-03
Thuraya-2	27825	RSO	152.710	0.556	2.639E-03	232.995	0.585	8.750E-04
Skynet-5B	32294	RSO	126.372	0.466	4.112E-03	251.333	0.492	2.435E-03
Skynet-5C	33055	RSO	84.290	0.228	1.317E-03	234.362	0.521	1.836E-03
Eutelsat-16A	37836	RSO	131.853	0.392	4.054E-03	215.793	0.561	2.205E-03
TDRS-12	39504	RSO	4665.285	3.933	8.750E-04	5188.430	3.614	2.630E-04
GPS-NAV-72	40294	REF	73.515	0.087	1.482E-02	179.656	0.202	3.553E-02
Telstar-12V	41036	RSO	197.636	0.361	3.011E-03	173.886	0.286	3.051E-03

For the use case scenario previously described, the time biases for each of the two EO sensors located in Southern Spain and South Africa were estimated in the multi-state filter which included one of the sensors (Southern Spain) tracking the GPS-NAV-72 reference satellite. It can be seen in Figures 29 and 10 that the biases converge to better than 1 millisecond for each of the sensors, though the Southern Spain sensor which tracks the GPS reference directly (Figure 29) converges after about an hour of EO measurements whereas the South African sensor timing bias (Figure 30) takes on the order of 3-4 hours to converge. This is likely due to the indirect link to the reference information which finds its way into the estimate via the correlations in the multi-state filter. This hypothesis is validated in the next section.

The multi-state filter was run for the 8-satellite, 2-sensor scenario for the two cases where the timing biases were estimated and, also, for when they were considered. This latter case would occur if a reference satellite (e.g. GPS) was not available. The pre-and post-fit residuals – a composite for all EO observations – is shown in Figure 31 for the case where the timing biases were estimated, and in Figure 32 for the case where they were considered. The latter residuals clearly show the systematic error resulting from the biased time-tags, primarily in the right ascension measurements. One or

more of the sensors also show a systematic error in the declination component, an artifact of how the filter converged for some of the tracked ROS's.

Two examples of the position state estimates for one of the "RSO" objects in the multi-state filter, in this case Skynet-5C, are provided in Figures 33 and 34 for the case where the timing biases were estimated (Figure 33) and considered (Figure 34). The state is seen to converge after about an hour for the case where the time biases are estimated (Figure 33) to the 10's of meters level, whereas the filter state takes several hours to converge and it's error versus the "truth" is on the order of 100's of meters (Figure 34). Note, though, that in both cases the errors remain within the 3- σ values as the result of the biases being considered rather than just simply ignored.

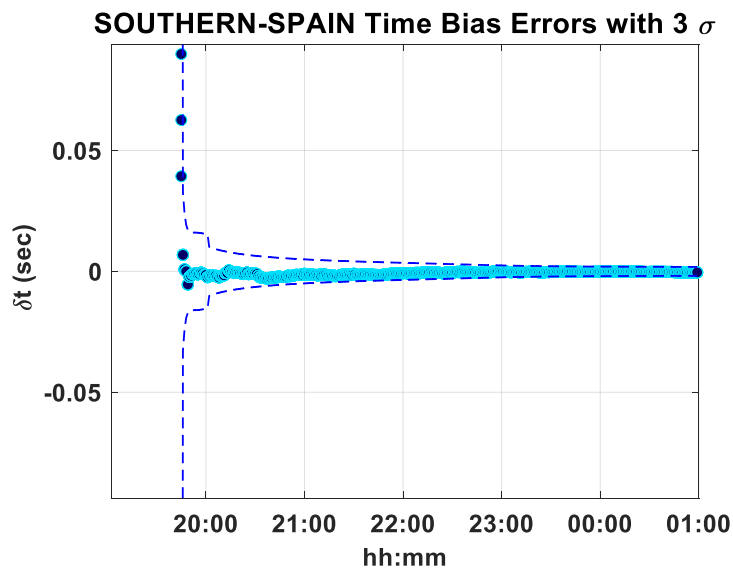


Figure 29. Southern Spain timing bias error and 3- σ uncertainty

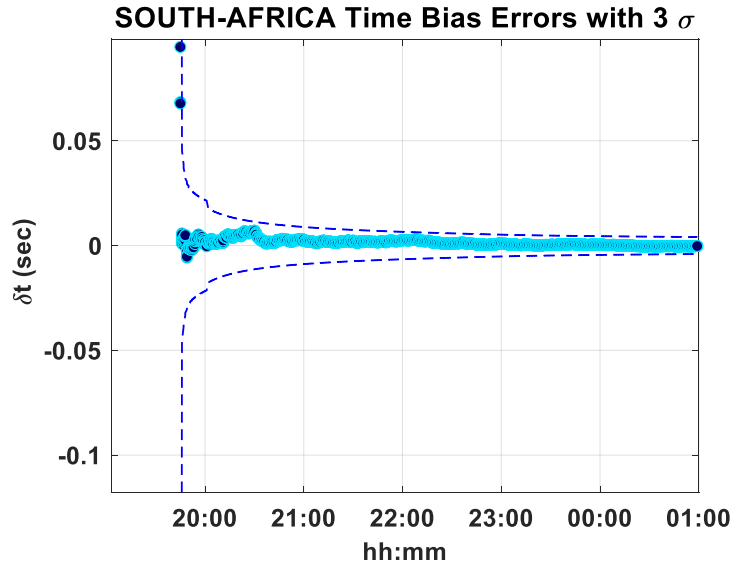


Figure 30. South Africa timing bias error and 3- σ uncertainty

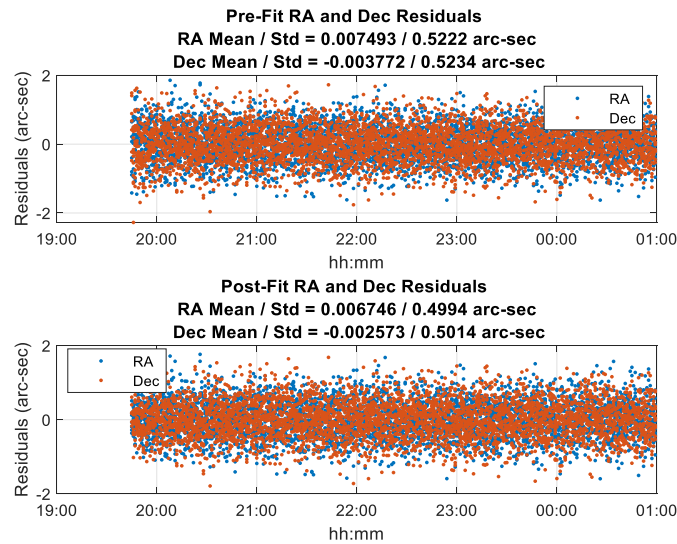


Figure 31. Pre and Post-fit residuals with timing bias estimated: Accurate IGU state included in the USKF updates

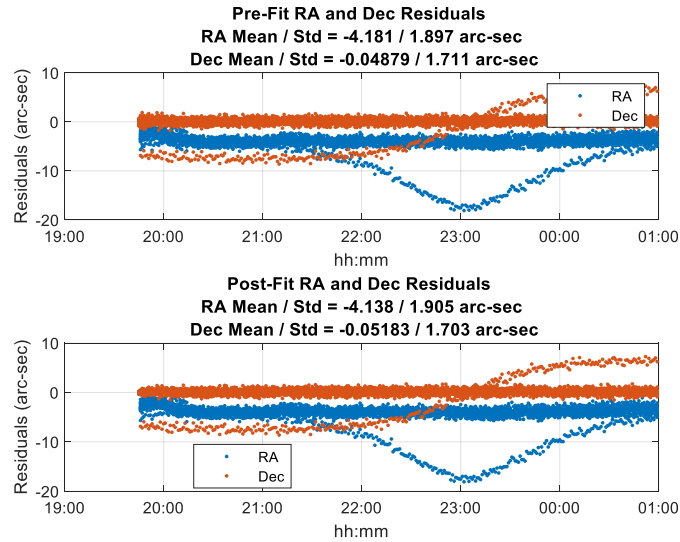


Figure 32. Pre and Post-fit residuals with timing bias considered estimated: Accurate IGU state included in the USKF updates

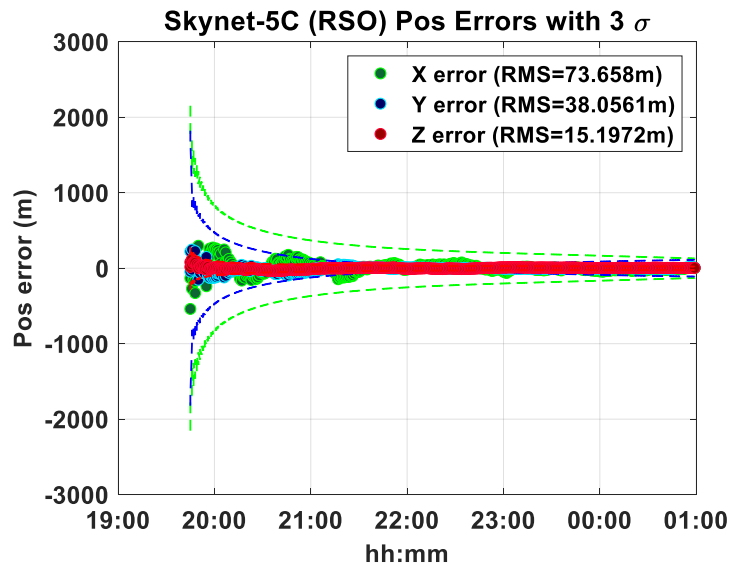


Figure 33. Skynet-5C (RSO) orbit position estimate error and 3- σ uncertainty: timing biases estimated

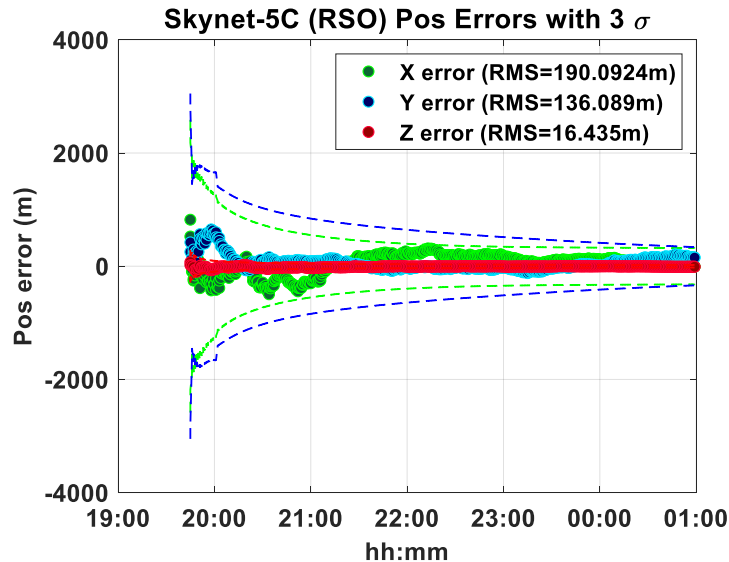


Figure 34. Skynet-5C (RSO) orbit position estimate error and 3- σ uncertainty: timing biases considered

8.3 Analysis Results for when No Reference Satellite is Included in the Filter

The 8-satellite, 2-sensor use-case analysis that was presented in the previous section was repeated, but without including the accurate IGU state for the GPS reference in the USKF measurement updates. A summary of results for this scenario is shown in Table 7 for the case where timing biases are estimated versus considered for the two optical sensors. It is clear, based on these results indicating hundreds of meters in error for each case, that the reference IGU states do indeed have a significant influence in producing accurate state estimates. Further, the pre-fit residuals for the “time bias estimated” case that are provided in Figure 35 shows indication the filter does its best to estimate states, but the fit is not good. Similarly, though the measurement residuals are somewhat worse in the case where they are considered as indicated in Figure 36, the filter estimates are similarly poor when compared to the known truth states for the 7 GEO satellites. This seems to imply the existence of an accurate truth state in the multi-state filter is crucial to its success in producing simultaneous time bias estimates and accurate satellite state estimates.

Table 7. Summary of estimated vs. consider from multi-state dynamic filter: No accurate IGU state included in the USKF updates

Sat Name	SSN i.d.	Type	Time Bias Estimated			Time Bias Considered		
			Pos Rss (m)	Vel Rss (m/s)	CrA/m Rss (m ² /kg)	Pos Rss (m)	Vel Rss (m/s)	CrA/m Rss (m ² /kg)
TDRS-9	27389	RSO	357.205	0.572	3.818E-03	460.793	0.429	2.549E-03
Thuraya-2	27825	RSO	352.293	0.260	2.198E-03	425.766	0.671	2.435E-03
Skynet-5B	32294	RSO	342.086	0.485	2.005E-03	427.777	0.320	7.457E-03
Skynet-5C	33055	RSO	383.888	0.455	4.076E-03	414.906	0.326	2.631E-03
Eutelsat-16A	37836	RSO	360.437	0.630	3.053E-03	409.606	0.254	2.144E-03
TDRS-12	39504	RSO	2469.786	6.169	9.060E-04	3007.738	9.319	1.073E-03
Telstar-12V	41036	RSO	370.043	0.606	6.822E-03	438.736	0.459	2.693E-03

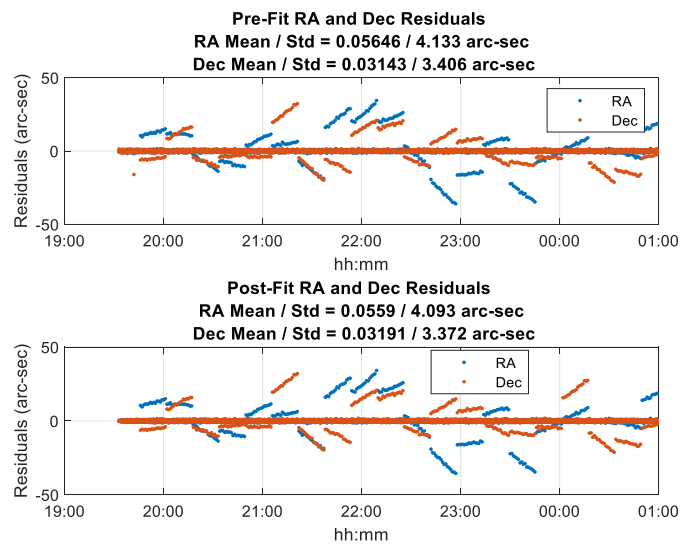


Figure 35. Pre and Post-fit residuals with timing bias estimated: No accurate IGU state included in the USKF updates

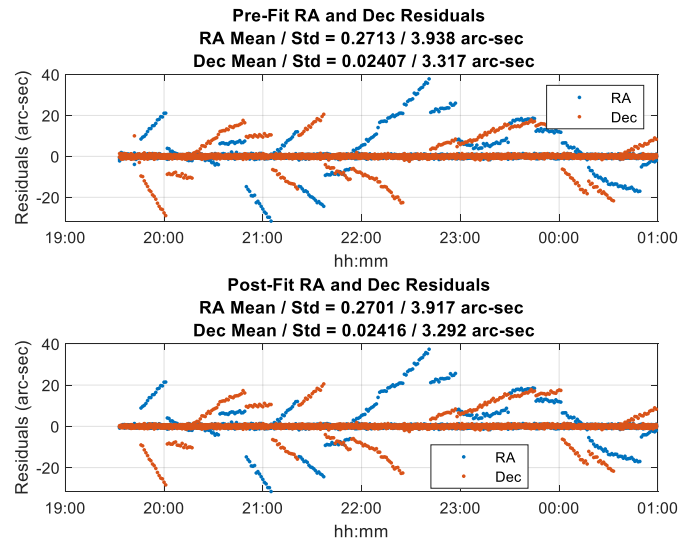


Figure 36. Pre and Post-fit residuals with timing bias considered: No accurate IGU state included in the USKF updates

9 Discussion of data management for automated real-time implementation

The O2 project established a data architecture that enabled a process to be developed and implemented for Department of Defence (DoD) purposes [18], and other parties such as the European Space Agency (ESA) are also endeavouring to establish an “Expert Centre” and associated infrastructure to manage and assess data quality and utility [19]. The intent of both concepts is for users of data to be able to have knowledge of the quality and integrity of the data they are using for Space Situational Awareness.

For the purpose of this research effort a cloud-based web presence and data repository was implemented for the storage and distribution of collected observations, allowing the storage and distribution of the data between the parties involved. While the information held within the repository is not classified, proper protection of the systems as well as restricted access to information is implemented.

As depicted in Figure 37, the web presence is used to support an interface for multiple customers and provides appropriate authentication, with varying authorization levels for access to information. The cloud implementation supports its own independent but highly-redundant data repository with accompanying storage and can be expanded in the future to incorporate processing capabilities

Mechanics meeting in January of 2019. These papers are included as deliverables as a part of this final report.

11 Transition and exploitation

There are several potential transition and exploitation opportunities the dynamic USKF filter developed from this research, including the United States Air Force (USAF) and other U.S. government entities.

By incorporating the dynamic USKF filter into the current Consolidated Space Situational Awareness (SSA) Operations Data Archive (CODA) architecture, CODA's capability is greatly enhanced. Currently, CODA supports operations in the National Space Defense Centre (NSDC). Future opportunities might include the 18th Space Control Squadron (SPCS) at Vandenberg Air Force Base (AFB), or other U.S. government organizations and facilities providing operational capabilities at higher security classification levels.

There are also very likely opportunities within L3-ADS to use the methods for in-house data processing to support other commercial SSA services.

12 Future work

We propose future work to accommodate dynamic calibration of radar sensor measurements for near real-time space object tracking and characterisation. It builds on the research presented in this report and would examine approaches for the dynamic calibration of radar sensor data, techniques for cross correlation of optical and radar measurements, and methods for determining sensor quality information, long terms trends and biases. Radio Frequency (RF) might also be included in a follow-up study to leverage the growing database of RF measurements and tracked reference satellites.

The introduction of new sensors, or the use of third party sensors, within the space situational awareness architecture is difficult and lengthy, often taking a number of years to introduce to the system. Techniques that would enable more rapid assessment of third party sensors, determination of sensor quality and integrity would enable external sensors to be utilised more readily and significantly improve the space operational awareness.

The proposed research activity would propose a team consisting of Applied Space, L3-ADS and LEOLABS and draw on radar data from the LEOLABS commercial network, avoiding classification issues

that would result from potentially using other radars such as Fylingdales. The results of the research would be equally applicable however to sensors operating on the classified domain.

13 Conclusions

The basis research project successfully investigated ways of performing independent calibration of electro-optic sensors, and created a foundation on which future activities can be built. A concept of implementation was developed using techniques that enable the calibration of third party electro-optic sensors, and to perform routine dynamic calibration to ensure the integrity and accuracy of the observational data. Taking such an approach a new sensor can be onboarded within a matter of days or sooner, rather than the months or years previously taken. More specifically, a near real-time dynamic calibration process was proposed and a prototype implemented which accommodates estimation of sensor related biases when reference data are also available; the biases can also be “considered” prior to estimation. A set of performance metrics can be used to determine filter performance and, subsequently, data specific performance metrics, to enable the dynamic process to be used appropriately. Improvements in the calibration process enable newly vetted sensors to be “trusted” and subsequently used to track non-reference satellites to sufficient accuracy so as to enable them to also be used as references for sensor calibration.

Improvements in the calibration process enable newly vetted sensors to be “trusted” and subsequently used to track non-reference satellites to sufficient accuracy so as to enable them to also be used as references for sensor calibration. The concept relies on tracking of GPS/GNSS “reference satellites” and access to IGU data which are posted regularly in near real-time. Other reference satellite sources may also be used, though the reference ephemeris data must meet accuracy and timeliness standards for the calibration. Additional work needs to be done to better understand the correlations between the EO sensors tracking the reference and those that do not. Likewise, additional scenarios that include “dynamic artefacts” will be constructed and analysed to demonstrate the viability of the technique to help distinguish between the two phenomena. Finally, future work will also demonstrate the concepts presented using actual EO and IGU data for representative satellites and sensors.

14 References

- [1] Limitations in availability of GEO operational slots:
<http://scholarlycommons.law.northwestern.edu/cgi/viewcontent.cgi?article=1216&context=njilb>
- [2] Space Track definition of GEO orbit regime: www.space-track.org
- [3] Number of operational satellites in the GEO orbit: <http://www.ucsusa.org/nuclear-weapons/space-weapons/satellite-database#.WRHcVojtPY>
- [4] Kelecy, T. and M. Jah, “Analysis of Orbit Prediction Sensitivity to Thermal Emissions Acceleration Modeling for High Area-to-mass Ratio (HAMR) Objects,” AMOS Technical Conference, Maui, HI, Maui Economic Development Board, 2009.
- [5] Vallado, D., Kelecy, T., and M. Jah, “Data Integrity in Orbital Data Fusion,” 63rd International Astronautical Congress. Naples, Italy: International Astronautical Federation, 2012.
- [6] Galeano, P., Joseph, E., Lillo, R. E.: The Mahalanobis Distance for Functional Data with Applications to Classification. Technometrics, Vol. 57, No. 2, pp. 281-291 (2015).
- [7] Wright, J. R., “McReynolds’ Filter-Smoother Consistency Test,” Internal Analytical Graphics Inc. white paper, May 15, 2009.
- [8] AstriaGraph Source:
<http://astria.tacc.utexas.edu/AstriaGraph/>
- [9] Kelecy, T and M. Jah, “Detection and orbit determination of a satellite executing low thrust maneuvers,” Acta Astronautica, Volume 66, Numbers 5-6, pp 798-809, March/April 2010.
- [10] Raley, J. et al, “The OrbitOutlook: Autonomous Verification and Validation of Non-Traditional Data for Improved Space Situational Awareness,” 17th Advanced Maui Optical and Space Surveillance Technologies (AMOS) Conference. Maui, HI: Maui Economic Development Board, 2016.
- [11] Hussein, I., M. P. Wilkins, C. W. T. Roscoe, and P. W. Schumacher, Jr., “On Mutual Information for Observation-to-Observation Association,” 25th AAS/AIAA Space Flight Mechanics Meeting, Williamsburg, VA, Jan. 11–15 2015.

- [12] Tapley, B., B. Schutz and G. Born, Statistical Orbit Determination, Elsevier Academic Press, 2004.
- [13] Kelecy, T., R. Knox and R. Cognion, "The Extended HANDS Characterization and Analysis of Metric Biases," AMOS Technical Conference, Wailea, Maui, HI Sept 16-19, 2008.
- [14] J. Stauch and M. Jah, On the Unscented Schmidt-Kalman Filter Algorithm. Journal of Guidance, Control, and Dynamics 38(1): 117-123, 2014.
- [15] X. Ning, F. Wang, and J. Fang, Implicit UKF and its observability analysis of satellite stellar refraction navigation system, Aerospace Science and Technology 54 (2016) 49-58.
- [16] G. P. Huang and S. I. Roumeliotis, An observability constrained UKF for improving SLAM consistency, Multiple Autonomous Robotic Systems Laboratory technical report number 2008-0002, August 2008.
- [17] S. M. Baker, C. H. Poskar, and B. H. Junker, Unscented Kalman filter with parameter identifiability analysis for the estimation of multiple parameters in kinetic models, EURASIP Journal on Bioinformatics and Systems Biology 2011.
- [18] Czajkowski, M. et al, "The Orbit Outlook Data Archive," 17th Advanced Maui Optical and Space Surveillance Technologies (AMOS) Conference. Maui, HI: Maui Economic Development Board, 2016
- [19] T. Flohrer, B. Jilete, T. Schildknecht and E. Cordelli, "First results from the deployment of Expert Centres supporting optical and laser observations in a European Space Surveillance and Tracking System," Proceedings of the 19th Advanced Maui Optical and Space Surveillance (AMOS) Technical Conference, September 2018.
- [20] Flohrer, C. (2008), "Mutual validation of satellite-geodetic techniques and its impact on GNSS orbit modeling," Zürich, Switzerland: Schweizerische Geodätische Kommission, Institut für Geodäsie und Photogrammetrie, Eidg. Technische Hochschule Zürich.

15 Acronyms and abbreviations

AAS – American Astronautical Society
AFOSR – Air Force Office of Scientific Research
CODA – Consolidated (SSA) Operations Data Archive
CONIMP – Concept of Implementation
CONOPS – Concept of Operations
DARPA – Defense Advanced Research Projects Agency
EO – Electro-Optical
EOARD – European Office of Aerospace Research and Development
ESA – European Space Agency
GEO – Geosynchronous Earth Orbit
GNSS – Global Navigation Satellite System
GPS – Global Positioning System
IAC – International Astronautical Congress
IGR – International GNSS Rapid Orbit Service
IGU – International GNSS Ultra-rapid Orbit Service
MD – Mahalanobis Distance
MEO – Medium Earth Orbit
NRT – Near Real-time
NSDC – National Space and Defense Center
O2 – Orbit Outlook
OD – Orbit Determination
RSO – Resident Space Object
SGP4 – Simplified General Perturbations
SSA – Space Situational Awareness
SRP – Solar Radiation Pressure
TDRS – Tracking Data and Relay Satellite
TLE – Two Line Element
UKF – Unscented Kalman Filter
USAF – United States Air Force
USKF – Unscented Schmidt Kalman Filter
WAAS – Wide Area Augmentation System

16 Annex – Conference and journal papers

International Astronautical Congress (IAC) oral presentation and paper:

Kelecy, T., E. Lambert, B. Sunderland, J. Stauch, T. Kubancik, V. Mallik, M. Jah, J. Paffett, N. Sanchez-Oritz, J. Nomen-Torres, “Automated Near Real-time Validation and Exploitation of Optical Sensor Data for Improved Orbital Safety,” 69th International Astronautical Congress (IAC), Bremen, Germany, 1-5 October 2018 (IAC-18,A6,10-C1.7,4,x46278).

Acta Astronautica Journal Article (derived from IAC paper):

Kelecy, T., E. Lambert, B. Sunderland, J. Stauch, V. Mallik and M. Jah, “Automated Near Real-time Validation and Exploitation of Optical Sensor Data for Improved Orbital Safety,” Acta Astronautica (AA_7265), DOI information: 10.1016/j.actaastro.2018.12.043, 8 January, 2019.

<https://www.sciencedirect.com/science/article/pii/S0094576518317247?via%3Dihub>

American Astronautical Society (AAS) Space Flight Mechanics oral presentation and paper:

Kelecy, T., E. Lambert, B. Sunderland and J. Stauch, “Automated Near Real-time Validation and Data Integrity Assessment using an Unscented Schmidt Kalman Filter (USKF),” 29th AAS/AIAA Space Flight Mechanics Meeting (AAS 19-521), Ka’anapali, Maui, HI, 13-17 January, 2019.